2024

Impact of the substrate stiffness on macrophage function

Aaron Newchurch

IMPACT OF THE SUBSTRATE STIFFNESS ON MACROPHAGE FUNCTION

Aaron Newchurch

A THESIS

Submitted in partial fulfillment of the requirements
for the degree of Master of Science
in
Chemistry
to
The Graduate School
of
The University of Alabama in Huntsville
May 2024

Approved by:

Dr. Anuradha Subramanian, Research Advisor
Dr. Bernhard Vogler, Committee Chair
Dr. Anuradha Subramanian, Committee Member
Dr. Carmen Scholz, Committee Member
Dr. Bernhard Vogler, Department Chair
Dr. Rainer Steinwandt, College of Science Dean
Dr. Jon Hakkila, Graduate Dean

Abstract

IMPACT OF THE SUBSTRATE STIFFNESS ON MACROPHAGE FUNCTION

Aaron Newchurch

A thesis submitted in partial fulfillment of the requirements for the degree of Master of Science

Chemistry

The University of Alabama in Huntsville
May 2024

This study explores macrophage cell function in healthy and diseased tissue that alters the synovial membrane housing fibroblasts and macrophages by examining how substrate stiffness impacts macrophage function. Current research suggests macrophages adapt, becoming more inflammatory in this environment. Divalent ions ($CaCl_2$ or $SrCl_2$) are used to adjust alginate hydrogel stiffness. The monocyte cell line THP-1 is transformed into macrophages through PMA, LPS, and IFNγ treatment within hydrogels, then cultured for 12 days. Divalent ions affect macrophage functionality; Sr^{2+} crosslinked hydrogels show higher viability, as well as an increased expression of M1 markers CD197 and IL1β, while M2 marker expression stays consistent for both ions. Ca^{2+} crosslinked hydrogels show higher secretion of MCP-1, IL1β, and TNFα, and persist longer compared to Sr^{2+} crosslinked hydrogels. Despite lower cytokine expression in Sr^{2+} crosslinked hydrogels, their viability and gene expression surpass Ca^{2+} crosslinked hydrogels. This suggests Sr^{2+} hydrogels promote M1 macrophages more effectively.

Table of Contents

List of Figures

List of Tables

Chapter 1. Introduction

1.1 Joints

A joint is the point at which two bones come into contact. The body has three types of joints named after their connective tissue: fibrous, cartilaginous, and synovial [1]. Fibrous joints contain mostly collagen for connecting the bones together making it very difficult to move and leaving the joint with no cavity. These joints include the skull, teeth, and the tibia-fibula connection. Cartilaginous joints contain hyaline cartilage or fibrocartilage as connective tissue and are often found around long bones and are slightly moveable. Cartilaginous joints are also common in the pelvis region of the body. Finally, the synovial joints, free-moving joints, are the main joints found in the body, crucial for joint movement [2]. These joints contain a joint cavity that holds the synovial membrane (synovium), the hyaline cartilage that covers the surface of both bones, and some synovial joints may contain menisci between the bones. These joints cover several joint mechanisms in the body, such as the hinge, saddle, planar, pivot, condyloid, and ball-and-socket joints. In addition to these joints having different cartilage structures, they have different forms of blood supply. Fibrous joints have their blood delivered through vessels branched off the artery. Cartilaginous joints receive blood to the periphery because cartilage is an avascular tissue and blood vessels do not enter the cartilage. Synovial joints receive blood from arteries that pass on either side of the joint, the periarticular plexus. In this study, we are focusing on the synovial joint at the knee by determining

how to promote macrophage healing in the thickened synovial membrane. Our interest in the knee joint is to determine a way to combat Osteoarthritis (OA), which impacts up to 528 million people worldwide, an increase of 113% since 1990. It is most prevalent in people aged 55 years and older. It is important to focus on the knee as it is the most frequently affected joint by OA, with a prevalence of 365 million cases impacting the knee joint [3].

1.2 Synovium

In this study, we focus on the synovial joint. We want to gain a better understanding of how the stiffening of the synovial membrane in the joint impacts the development of macrophages. The synovium contains layers, the first is a thin layer of fluid composed of tissue macrophage A cells, fibroblast B cells, and fenestrated capillaries. Surrounding this layer is a protective thicker layer of loose connective tissue called the sub-synovium, also containing transport vessels. Finally, there is a layer surrounding the connective tissue called the extracellular matrix, containing collagen, hyaluronan, and fibronectin [4]. The synovial membrane is a thick membrane surrounding the synovial joint that acts as a source of nutrients. Extremely filtered blood plasma makes up the synovial fluid, this blood is then further filtered once entering the synovial membrane. This blood can then supply the synovial joint nutrients and immune cells when under stress. The synovial joint is prone to injury in a few different ways. The most common form of injury is Osteoarthritis (OA), which is a form of arthritis that wears down the cartilage in joints. Contact injuries, stress injuries, obesity, or age can cause OA, and OA can affect the hands, knees, hips, or spines. Single acute impact or repetitive cumulative impact leads to OA. These impact injuries lead to cartilage

releasing reactive oxygen species (ROS) from the mitochondria. ROS causes chondrocyte death and synovial matrix degradation [5]. Obesity can lead to OA through factors such as adipose deposition, insulin resistance, and improper immune response [6]. These factors lead to over-recruitment of inflammatory cells into the synovial joint. Lastly, age is a cause of OA development. As you age, your cartilage becomes dryer and stiffer, leading to degradation. By the age of fifty, there are observable radiographic signs of OA, such as the narrowing of joint spaces and osteophytes (bone growth into the joints), start to appear. Studies have also shown that in aging bovine meniscus there is a decrease in the repairability of the tissue. Additional studies show an increase in pro-inflammatory markers in the meniscus of humans over 40 years old. Our study wants to provide a better understanding of how macrophages can develop in these areas and help repair the injured tissue through macrophages [7].

Metabolic studies have furthered the understanding of how age impacts OA. These studies show that aging and mitochondrial damage both lead to an increase in ROS production, which prolongs the production of pro-inflammatory cytokines [8]. They found that there are several metabolites that contribute to inflammation and cartilage damage, leading to the development of OA. Nitric Oxide is the main metabolite found to be elevated in patients with pro-inflammatory macrophages and OA. Furthermore, there is an increase in Prostaglandin E2 (PGE2) pain signalers found in the patient's synovial membrane. PGE2 signaling enhances the production of NO, thus further promoting pro-inflammatory response in the body. Furthermore, people with developing OA have increased levels of lactic acid in the joints. Lactic acid is a key component in the intracellular signaling pathway that controls pro-inflammatory cytokine production [9].

This response promotes inflammation in the synovial membrane and results in the inability to quickly provide monocytes to the joint.

The synovium contains many types of cells with macrophages being the most abundant at 12-40% of the synovial immune cells. Other major cells in synovium include synovial fibroblasts and infiltrating T lymphocytes, while it also contains smaller concentrations of B lymphocytes, dendritic cells, plasma cells, mast cells, and osteoclasts [10]. The macrophages play the most crucial role in the synovial membrane by maintaining joint homeostasis clearing out debris and promoting tissue repair. A proposed therapeutic approach to target OA is the distribution of pro-inflammatory macrophages into the synovium. This proposition comes from a study that used macrophage-depleted synovium through the injection of anti-CD14. This study showed there was a decrease in IL-1β, TNF, and matric metalloproteinases (MMPs), as well as a reduction in cartilage damage and osteophyte formation [8]. To further understand why there would be a need for macrophage therapy rather than allowing the body to naturally heal, there needed to be a better understanding of what happens between macrophages, and the synovium as it stiffens. The thickening of the synovial membrane inhibits the mobility of the macrophages, preventing macrophages from entering the synovial fluid and attacking the areas of inflammation or injury, causing OA to develop without a chance of healing. As the synovial membrane thickens macrophage phenotypes and cytokine secretion patterns begin to change, leading to chronic inflammation and tissue damage. These results are evident in a study that found that macrophages exposed to thickened synovial membrane express an increased concentration of pro-inflammatory cytokines, such as TNFα and IL-1β [11]. Since there is an increase in pro-inflammatory

cytokine secretion, there is an imbalance of pro and anti-inflammatory factors needed to promote healing, and if pro-inflammatory cytokines are overexpressed, then chronic inflammation can occur, blocking the healing phase from starting. Currently, there is no study into macrophages' development through varying stiffness of media, making this study necessary to gain a better understanding of how we can promote macrophage polarization in stiffer environments for optimal healing in these harsh joint environments. In this study, we will determine how the varying thickness of the synovial membrane plays a role in macrophage polarization and development.

1.3 Macrophages

To understand how hydrogels impact the polarization of macrophages, you will first have to understand how macrophages develop and polarize on their own, outside of environmental effects. As a monocyte develops into a macrophage, it goes through several stages, which have their own characteristics. The monocytes are leukocytes that come from stem cells in the bone marrow and circulate in the bloodstream. Monocytes are the precursors to macrophages and can differentiate into different types of macrophages based on the microenvironment. The monocyte will first differentiate into M0 macrophages, the resting state of macrophages. M0 macrophages can process phagocytes by engulfing and clearing foreign debris and apoptotic cells. M0 macrophages also help in the tissue repair process by clearing out the apoptotic cells and secreting matrix metalloproteinases (MMPs) for extracellular remodeling, and by producing growth factors promoting tissue regeneration [12]. These M0 macrophages further differentiate into M1 macrophages, activated macrophages. Pro-inflammatory stimuli, interferon-gamma (IFN-γ), lipopolysaccharide (LPS), and tumor necrosis factor-alpha

(TNF-α), impel M1 macrophages. M1 macrophages upregulate pro-inflammatory cytokines (IL-1β, TNF-α, and more), reactive oxygen species (ROS), and enhance antigen presentation. These macrophages express inducible nitric oxide synthase (iNOS), which catalyzes the production of nitric oxide (NO) [13]. NO plays a role in the microbicidal activity of M1 macrophages involved in killing intracellular pathogens. M1 macrophages can then further differentiate into M2 macrophages, activated macrophages, by induction of anti-inflammatory or tissue-repairing signals. M2 macrophages will produce high levels of interleukin-10 (IL-10), transforming growth factor-beta (TGF-β), and interleukin-4 (IL-4) [14]. IL-10 is an anti-inflammatory cytokine that inhibits pro-inflammatory cytokine production. TGF-β is a part of tissue repair and immunoregulation. Lastly, IL-4 promotes the activation of M2 macrophages leading to tissue repair and remodeling [15].

It is important to know about the pathway macrophages take to develop to better understand why macrophages are important and how their role differs from monocytes. Macrophages are immune cells scattered throughout the body in various tissues and organs and play a central role in innate and adaptive immunity. They can eliminate pathogens, cellular debris, and foreign substances. They can vary in size depending on their microenvironment but range between 10 and 30 micrometers. Macrophages can migrate and enter tissues; however, macrophages' shape depends on the tissue they are trying to enter, varying from round, elongated, or dendritic [16]. Initially, these macrophages enter the tissues as monocytes from the bloodstream. Subsequently, in response to factors such as the expression of colony-stimulating factors and cytokines, the monocytes undergo differentiation into macrophages. During differentiation, the

monocytes undergo a change in their gene expression, surface marker expression, and functionality. This differentiation process involves the activation and repression of specific signaling pathways to drive macrophage differentiation and polarization [15].

Macrophage's ability to heal wounds happens when the macrophage polarizes into its pro-inflammatory stage, M1, where it produces nitric oxide, ROS, IL-1, IL-6, and TNF-α. In addition to these compounds, M1 macrophages also secrete MMP-2 and MMP-9 that break down the extracellular matrix of cells. After this occurs, the M1 macrophages polarize into M2 macrophages, healing macrophages, where they start secreting growth factors such as PDGF, insulin-like growth factor 1 (IGF-1), VEGF, and TGF-β [17]. These growth factors are responsible for cellular proliferation, angiogenesis, and granulation tissue formation. While secreting these growth factors, M2 macrophages repress MMP-2 and MMP-9, so the extracellular matrix can reform, thus repairing the cell.

Monocytes are immune cells that circulate in the bloodstream and serve as a precursor to macrophages. Monocytes have different gene expression levels from a macrophage, making identification of a monocyte's differentiation into a macrophage identifiable. A monocyte's gene expression allows it to migrate, attach, and promote an inflammatory response in the body. An example of one of these gene markers is CCR2, which facilitates the recruitment to sites of inflammation and tissue injury [18]. Macrophages have a diverse and changing gene expression program to regulate their function, plasticity, and response to their microenvironment [12]. They also express various genes involved in phagocytosis, antigen presentation, cytokine production, and tissue remodeling, such as CD14 and CD68. Furthermore, macrophages produce various

cytokines and growth factors, such as TNFα, IL-1β, and TGF-β, which influence immune cell activation, inflammation, and tissue repairs [15].

Cluster of Differentiation (CD) markers are another commonly used way to identify the stage in the macrophage cycle. CD markers are the macrophage surface antigen expression and differ in their expression between each stage. CD14 and CD68 are CD markers commonly found in all types of macrophages, whereas CD11b is a tissue-specific marker for monocyte-derived macrophages, CD 169 is for splenic macrophages, and IL-4 and IL-13 activate the expression of CD206 in macrophages [19]. CD markers can be up-regulated or down-regulated based on the stage of development the cell is in. CD14 is a marker that gets up-regulated on monocytes but then down-regulated once differentiation into macrophages occurs. CD163, on the other hand, is a marker that is upregulated in macrophages. Its role is in the hemoglobin-haptoglobin complex and indicates when a macrophage differentiates into an M2 macrophage [20]. The stage of the macrophage also regulates markers. C-C chemokine receptor type 7, CCR7, also known as CD197, is an M1-specific marker as it is a ligand-specific marker that gets activated when inflammation is present [21]. The measuring of markers is important for determining the macrophages' stage in development, as distinguishing from phenotype alone is difficult and unreliable. This complication is because the macrophage can change its shape to adapt to the environment, which leads to M1 macrophages changing their shape to match more of an M2 macrophage [12].

1.4 THP-1 and U937

THP1 and U937 are the common monocytic cell lines used as precursors to macrophages. U937 cells derive from the histiocytic lymphoma of an adult male patient.

U937 cells are mature bone marrow-derived monocytes that, by culturing, double every 48 to 72 hours, making them a useful model for macrophages. However, the THP-1 cell was better suited for our lab because the cell does not need an affiliation with a hospital, and because altering the polarization pathways is easier since they are unmatured. Experiments commonly use the THP-1 cell line to represent macrophage biology and immune responses. This common use is because the human monocytic leukemia cell line derives from the THP-1 cell line, which can differentiate into macrophage-like cells when exposed to treatments like phorbol 12-myristate 13-acetate (PMA) [22]. After differentiation, the THP-1 representative of macrophages shares many characteristics of mature macrophages, such as morphology, functionality, and expression of surface markers. Differentiated THP-1 cells can represent several of the mature macrophage surface markers, such as CD11b, CD14, CD163, and CD206 [23]. Furthermore, differentiated THP-1 cells exhibit phagocytic activity as macrophages. Enabling them to engulf and eliminate foreign bacteria, cellular debris, and apoptotic cells. THP-1 differentiated cells can also secrete macrophage cytokines and chemokines, such as TNF-α, IL-1β, IL-6, and IL-10. THP-1 differentiated cells exhibit many of the widely accepted macrophage characteristics, making the THP-1 cell line an accurate model for macrophage studies into biology and immune response.

1.5 Hydrogels

Culturing of cells is often done in vitro on 2D substrates, such as petri dishes and culture plates. However, 2D petri dishes or culture plates cannot model 3D networks that include highly porous structures. For this reason, the use of hydrogels is a common structure for modeling these 3D networks because they provide the supporting

scaffolding needed to culture cells and mimic external environments [24]. Since hydrogel's physical and chemical properties can be easily modified, it makes it ideal for replicating different parts of the body. Chemicals can modify hydrogels to resemble hydrophilic networks like the physical properties of the extracellular matrix. The polymers that make up the hydrogels can also absorb large amounts of water and resemble fluid transport mechanisms. The mechanical properties of hydrogels are also easily modified through the density or bonding strength of crosslinking agents, providing variability in the regions of the body you are trying to mimic. If the area is soft, the hydrogel's stiffness should be low, and if the area is hard, the stiffness should be high. In our experiment, we are trying to mimic the highly thick and stiff synovial membrane surrounding the joint. We are also trying to determine how the thickening of the synovial membrane impacts the macrophages. For this, we need to control the stiffness of the hydrogel and vary it through crosslinking agents. Hydrogels are used for cell culturing and are commonly made up of natural biodegradable polymers that exist in life forms. Examples of these polymers are Collagen, chitosan, or alginate, which can be found in human bodies, the exoskeletal structure of crustaceans, or in brown seaweed, respectively.

Studies have tested if macrophages can be cultured in hydrogel. Studies have found that Poly (ethylene glycol) PEG-hydrogels can encapsulate macrophages without rejection due to a foreign body [25]. Hydrogel's capability for modification gives them the edge over ex vivo applications and allows for macrophage promotion [26]. Hydrogels also possess the ability to mimic local cues that would be native to cells' environments.

Hydrogels support cellular attachment, proliferation, and engulfment, providing an alternative to long cultures that encapsulate into the target locale [24].

Alginate is a biodegradable polysaccharide derived from brown seaweed. It has many uses in the medical, food, and biological fields due to its crosslinking structure and biodegradable nature. Alginate's structure comprises chains of (1-4)-linked β-D-mannuronic acid (M) and α-L-guluronic acid (G) residues. The ratio between M and G units varies in each alginate sample [27]. Changing the M: G ratio impacts the physical and chemical properties of the alginate. The M-block allows more solubility and viscosity, while the G-blocks provide rigidity and gel-forming properties to the structure. When divalent cations, such as calcium (Ca^{2+}) or strontium ions (Sr^{2+}), react with alginate it will start to gel. The hydrogel forms due to crosslinking between the alginate and the divalent cation leading to a polymer formation. Junctions, or pores, will form between the G-blocks binding together in a web-like bonding structure [28]. Modification of alginate's crosslinking is done by changing the concentration of alginate, the concentration of divalent cation in solution, or the molecular weight of alginate. In this crosslinking, alginate is used as a scaffold in tissue engineering, as it provides a 3D environment to seed cells. Differences in the M: G ratio, concentration of alginate or ions, and molecular weight enhance alginate's ability to perform cell adhesion, migration, or differentiation [29]. These modifications will allow for the representation of bone cartilage and vascular tissue regeneration.

Crosslinking occurs when alginate is in the presence of a divalent cation. This process results from the interaction between the carboxyl groups of alginate and the divalent cation. The carboxyl group (-COO-) of alginate will bind to the divalent cation

and form a coordination bond, resulting in a crosslinking pattern commonly referred to as the "egg-box" model [28]. Modifications to the concentration of alginate or divalent ions in a solution will change the number of interactions and affect the kinetics of the crosslinking changing the gelation and viscosity of the gel formed [27].

When the synovium membrane stiffens, the monocytes have difficulty entering the synovial fluid to polarize into macrophages, making the healing process slow or unachievable. Our study will give a better understanding of how to promote the polarization of macrophages in stiffer environments. This study will attempt to seed monocytes into hydrogels that contain different crosslinking agents. This change in crosslinking agents is to mimic the stiffening joint environment. Calcium, Ca^{2+}, and strontium, Sr^{2+}, are the crosslinkers used as they vary in atomic weight and are divalent ions that bind well to alginate's MG-block complex. Measuring the gene expression, survivability, and RNA concentration of the macrophages as they grow in these hydrogels will give answers to how the differing environments impact the polarization of the macrophages and help in the development of treatment options using macrophage therapeutics. To determine if there is a difference in the hydrogel environments, we will test the physical properties of the hydrogel, their storage (elastic) modulus, loss (plastic) modulus, and their pore sizes.

There is currently research into how ions impact alginate crosslinking. In a research study testing Ca^{2+}, Sr^{2+}, and Ba^{2+} against alginate, they found that the Sr^{2+} and Ca^{2+} ions performed evenly regarding maintaining alginate hydrogel structure [30]. A different study found that Sr^{2+} possessed better crosslinking with alginate and strong binding at each crosslinking site than Ca^{2+} ions [31]. This was concluded through various

test, including scanning electron microscope imaging of alginate fibers with Sr^{2+} and Ca^{2+} that found that the rate and degree of crosslinking impacted the morphology of the hydrogel, with Sr^{2+} creating a more porous and tighter crosslinked hydrogel than the Ca^{2+} ions. There have been studies preformed on alginate's stiffness and how it impacts the inflammatory response of macrophages, however, that study manipulated alginate's stiffness through adjustment of methacrylate–gelatin concentrations rather than through a change of crosslinking agents [32]. This study found that the increase in stiffness of the hydrogel induced cells to spread throughout the hydrogel. They also concluded that the increased stiffness of the hydrogel caused more nitric oxide synthesis on the macrophages, promoting M1 development. In this study, we aim to enhance the understanding of how crosslinking agents influence the inflammatory response of macrophages and contribute to their development.

Chapter 2. Material and Methods

2.1 Scanning Electron Microscope (SEM) Hydrogel Preparation

The morphology of the hydrogel's pore structure was viewed under SEM. After hydrogels were removed from the media, they were washed in room temperature phosphate buffered solution (PBS) for 24 hours. After the wash, the hydrogels were slowly cooled down to -20℃ from room temperature over 3 hours, before being frozen down to -80℃ over 24 hours. The hydrogels were then placed in a lyophilizer to dehydrate further at -60℃ and in a vacuum. The hydrogels were then coated with a Gold/Palladium compound using a sputter and examined under a Zeiss LEO 1550 SEM at The University of Alabama in Huntsville (Frank Berisford, The Center for Applied Optics, UAH).

2.2 Scanning Electron Microscope Image Analysis

The images were provided in a .tif format from The Center for Applied Optics, UAH, and imported into ImageJ™ software. The scale was calibrated using the provided scalebar. All pores were measured once using the longest diameter as shown in Figure 9. Pore diameter was then averaged across 27 pores (n=3) and represented as a categorical scatterplot.

2.3 Hydrogel Preparations for Rheology

A mold was made around a 35 mm disk in a 70 mm petri-dish by pouring 1% Agarose containing wither 500 mM $CaCl_2$ or $SrCl_2$ that was autoclaved prior to pouring. The gel was allowed to crosslink around a 35 mm diameter disk for 1 hour at room temperature, so that it would create a well. On the same day, the mold was made, the sample hydrogel disk solution, filtered, using a PTFE filter (Thermo Scientific, 42225-NN, 0.2 μm), 1.2% Alginate and 500 mM $CaCl_2$ or $SrCl_2$, was made and poured into the wells. Hydrogel disks were left to crosslink with the ions for 1 hour at room temperature in the wells before carefully removing, washing, and placing in DiH_2O. Mechanical properties of the hydrogel disk were measured on day 0, 3, 7, and 14 in triplicates. Procedure diagramed in Figure 5 and timeline in Figure 6.

2.4 Rheology

Hydrogels were placed on the rheometer, Haake Mars Modular Advanced Rheometer System Typ 006-3098, with a 35 mm cone shaped, 1˚ angle, Drehkorper/ Rotor P35/Ti/SE 222-2092. The plate was heated to 37°C and the probe was lowered until the entire surface of the hydrogel was touching the probe. The following settings were used to measure the G' and G" of the hydrogel: Frequency, 1.0 Hz; Stress, 0.5ϑ₀; and time, 180 seconds. Three such replicates from three independent experiments were used for analysis (n = 3). The software used to measure the G' and G" of the hydrogels was HAAKE RheoWin.

2.5 Suspension of THP-1 Cells

Blood derived cells from a 1-year-old male with acute monocytic leukemia, THP-1 (Lot# 70025047, Cat# TIB 202), were received from the ATCC and immediately placed in liquid nitrogen, -196°C, until use. Each vial of cells received contained 5.0 x 10^6 cells. The cells were thawed, counted, and then expanded in a T-75 flask containing RPMI-1640 medium (ATCC 30.2001) and the media composition was as follows: To make complete growth medium to support cell growth it should be supplemented with 10% FBS and 1x Penicillin-Streptomycin. The cells were counted every two days until the desired cell population was achieved. These THP-1 cells were used in later experiments.

2.6 Encapsulation of THP-1 cells in Alginate Hydrogels

Agarose molds were prepared by making 1% Agarose containing either 500 mM $CaCl_2$ or $SrCl_2$ then autoclaving, before pouring into a 70 mm diameter petri-dish so that the final height of the gel was 5 mm. After the gel was crosslinked for an hour at room temperature, a 5 mm biopsy punch was used to make wells 5 mm in diameter and 5 mm in height into the gel. On the same day as the making of the mold, a solution of filtered 1.2% Alginate and $2.73x10^6$ THP-1 cells per mL, cultured in methods section 2.5, were added to each well at 110 µL per well so each hydrogel contained $3x10^5$ cells. After hydrogel encapsulated cells were crosslink for 1 hour they were carefully removed and added to RPMI-CM/SM media in 6-well tissue culture plates (TCP), six hydrogels per well (n=8 plates) and incubated at 37°C and 5% CO_2. The RPMI-CM/SM media was composed of RPMI-1640 medium (ATCC 30-2001), 10% FBS, 1x Penicillin-

Streptomycin, 1.26 mM $CaCl_2$ or $SrCl_2$, and 400 mM $MgSO_4$. Hydrogels were cultured for three days in RPMI-CM/SM. The protocol schematics are represented in Figures 7 and 8.

2.7 Differentiation of Hydrogel Encapsulated THP-1 cells into Macrophages

Using the hydrogel encapsulated THP-1 cells cultured in methods section 2.6, PMA was added at 128 ng/mL (100 nM) to RPMI-CM/SM to each well, 4 mL of media per well. The THP-1 cells were differentiated to M0 macrophages through 72 hours of PMA incubation at 37°C, 5% CO_2, and 95% humidity. Fresh complete culture media, 4 mL, was added to each well. The cells rested for 72 hours at 37°C, 5% CO_2, and 95% humidity.

Polarization of M0 to M1 macrophages was attained through treatment of interferon gamma (IFNγ) followed by LPS induction. Fresh media containing 20 ng/mL of IFNγ was added at 3 mL per well and incubated at 37°C, 5% CO_2, and 95% humidity for 24 hours. After 24 hours of incubation, 1 mL of 80 ng/mL of LPS containing media was added to each well. This made the final concentration of LPS 20 ng/mL. The cells grew for another 48 hours at 37°C, 5% CO_2, and 95% humidity so they could differentiate into M1 macrophages. Finally, a continuation of fresh complete culture media addition occurred every 72 hours until 12 days was reached.

2.8 Live/Dead

Cell-seeded scaffolds were treated with LIVE/DEAD® Viability/Cytotoxicity Kit (Invitrogen), 2 µL/mL of green-fluorescent calcein-AM and 1 µL/mL of red-fluorescent ethidium homodimer-1 in 1 mL of Hank's Balanced Salt Solution, HBSS-CM/SM,

supplemented with 1.26 mM $CaCl_2$ or $SrCl_2$ and 400 mM $MgSO_4$, for 30 minutes in the dark at 37°C. The hydrogels were then washed three times with HBSS-CM/SM for 10 minutes each in the dark at 37°C and visualized using TexasRed (617 nm) and GFP (517 nm) with Lionheart Automated Fluorescence Microscope (BioTek Instruments, Model# 1908078). All the images were collected at 4x and 20× magnification.

2.9 Extraction of RNA from Hydrogels

Hydrogels were removed from media, 5 hydrogels were pulled from two wells in the 6-well TCP for a total of 10 hydrogels per group (n=3), and washed with Hanks' balanced salt solution (HBSS) (ThermoFisher) then added to dissolution buffer in a 15 mL conical tube at 37°C. The tube was then centrifuged at 120g for 30 seconds into a 1.5 mL Eppendorf tube at 700 μL increments. The supernatant was aspirated off and the pellet was dissolved in Trizol reagent (Invitrogen) for 5 minutes. Chloroform was added to the Trizol solution and mixed. The Eppendorf tube was then centrifuged to separate the layers. The PureLink™ RNA Mini Kit (Invitrogen, Lot# 12183018A) was used to wash the RNA sample of impurities. The integrity and purity of isolated RNA was then assessed by a nanodrop at A260/A280 nm absorbance ratios.

2.10 Reverse Transcription Polymerase Chain Reaction (RT-PCR)

Using the RNA data from the extraction of RNA from hydrogels (2.9), the volume of RNA needed for RT-PCR cycle could be calculated. The RT-PCR solution contained, TaqMan® RT-PCR Mix (2X) (Life Technologies, USA), Taq Man®RT Enzyme Mix (40X) (Life Technologies, USA), RNA Sample, Nuclease Free water, and the primer (ITGAM (Hs00167204_m1), CCR2 (Hs01013469_m1), CD163

(Hs00174705_m1), CD197 (Hs01013469_m1), and IL1β (Hs01555410_m1)). This solution was mixed, centrifuged at 170 rcf for 5 minutes, then placed in the RNA reader. The RNA reader was set to the following thermal cycle conditions: Stage 1, hold at 48℃ for 15 minutes; Stage 2, hold at 95℃ for 10 minutes; Stage 3, cycle at 95℃ for 15 second; Stage 4, cycle (40 times) at 60℃, for 1 minute. The expression of mRNA transcripts was normalized to the housekeeping gene, GAPDH (Hs02786624_g1); expression and relative expression levels were calculated using the $2^{-\Delta\Delta Ct}$ method.

2.11 Enzyme-Linked Immunoassay (ELISA)

The concentration of CCL2 (MCP-1), TNFα and IL1β (Cat# DY279, DY210-05, DY 201-05) in various samples was determined by ELISA. The 96-well TCP was coated with 200 µL of capture antibody (lot# GY4022033) per well, sealed to prevent evaporation, and incubated overnight at room temperature. The plate was washed with phosphate buffered solution and 0.005% Tween (PBS-T), and blocked with reagent diluent, 1% bovine serum albumin in PBS, was added at 300 µL per well for an hour at room temperature. The 96-well TCP was washed again. The standard curve for CCL2 was made in the range of 1000 – 15.6 pg/mL, TNFα was made in the range of 1000-15.6pg/mL, and IL1β a range of 250-3.91 pg/mL was prepared using the standard solution that was provided in the ELISA kit. The samples and standard were loaded at 100 µL per well and incubated for 2 hours at room temperature, each sample was loaded as n=3. The plate was washed again and 100 µL of detection antibody (lot# UB3822041) was loaded in each well. Plate was washed once more and 100 µL of Streptavidin-HRP (lot# P330988) was added for 20 minutes at room temperature in the dark. The plate was washed one more time. Finally, 100 µL of substrate solution, 1:1 mixture of Color

reagent A (H_2O_2) and Color reagent B (Tetramethylbenzidine), was added to each well for 20 minutes in the dark, then immediately 50 µL of stop solution, 2N H_2SO_4, was added and thoroughly mixed, and the optical density was determined at 450 nm using a Microplate reader, BioTek 800TS at UAH.

2.12 Statistical Analysis

The graphs were generated using GraphPad Prism software. Quantitative results were analyzed using a two-way ANOVA Ordinary comparison test, ns represents non-significant, * represents p value >0.01, ** represents p value <0.01, *** represents p value <0.001 and **** represents p value <0.0001. Data were represented as the average of all groups ± standard error (SE) over a sample number of n.

Chapter 3. Results

3.1 Scanning Electron Microscopic (SEM) Comparison of Sr^{2+} and Ca^{2+} Crosslinked Hydrogel Pores

The SEM images taken by Frank Berisford at the Center for Applied Optics; UAH were captured as .tif files. These files were processed using ImageJ™ software, as shown by the representative image in Figure 9, panel C-F. The scale of the lines was first calibrated using the scalebar provided by the .tif image. Each pore was measured once using the longest portion of the pore. The average pore size of each group of hydrogels was determined from 27 pores per hydrogel for three separate hydrogels, Figure 10. The average pore size of the M1D0 hydrogels made with Sr^{2+} and Ca^{2+} was 48.80 ± 17.59 and 75.92 ± 33.58 μm, respectively. Upon continued culture of M1 macrophages for another 12 days, the following pore sizes were noted for Sr^{2+} and Ca^{2+}, 114.33 ± 67.97 and 106.37 ± 66.79, respectively. Preliminary observations indicate that the average pore size of Ca^{2+} hydrogels were larger than the Sr^{2+} crosslinked hydrogels. Pores, 27, were measured as n=3. Hydrogels before M1 development and hydrogels without cells did not contain any pores. Data were analyzed using a two-way ANOVA comparison, with $p < 0.05$.

3.2 Rheological Analysis of Sr^{2+} and Ca^{2+} Crosslinked Hydrogel's Retention to Deformation

The rheological data collected from the hydrogels, Figure 11, shows Ca^{2+} G' had a lower retention pressure than Sr^{2+} on day 0, Sr^{2+} was 816.08 Pa and Ca^{2+} was 360.14Pa. However, Ca^{2+} crosslinked hydrogels continued to increase their G' value over the 14-day culture and reached a value of 1159.41 Pa compared to Sr^{2+} day-14 value of 911.58 Pa. For both Sr^{2+} and Ca^{2+} crosslinked hydrogels the G" value was not significantly changed throughout culturing. Each measurement represents n=3, with 20 measurements being recorded by HAAKE RheoWin software for each sample.

3.3 The Viability of Monocytes and Macrophages Cultured in Sr^{2+} and Ca^{2+} Crosslinked Hydrogels

The live/dead imaging of Sr^{2+} and Ca^{2+} crosslinked hydrogels was captured using Lionheart Automated Fluorescence Microscope (BioTek Instruments, Model# 1908078), and analyzed with its software to count the total number of live and dead cells, Figures 12 and 13. These data shows that the Sr^{2+} crosslinked hydrogels maintained a higher viability of macrophage cells (M1), average percent alive 85.32, than the Ca^{2+} crosslinked hydrogels did, average percent alive 67.50. This data represents 2 hydrogels, each from a different well of a 6-well TCP plate. The results were analyzed using a two-way ANOVA comparison, $p > 0.005$.

3.4 The Impact of Sr^{2+} and Ca^{2+} Crosslinked Hydrogels' have on Protein Expression of Macrophages

In the Sr^{2+} crosslinked hydrogels, the concentration of monocyte chemoattractant protein 1, MCP-1, (Early M1 macrophage marker), IL1β, Interleukin-1 beta, (M1 macrophage and an inflammatory cytokine marker), and TNFα, Tumor necrosis factor alpha, (M1 macrophage marker) in the cell culture media over various days was determined by the ELISA procedure, Figure 18. Expression of MCP-1 was significantly upregulated, 400-fold from THP-1 monocytes to M1D0 macrophages during culturing, but then had zero expression over the 12-day M1 culturing of Sr^{2+} crosslinked hydrogels. Similarly, IL1β expression was significantly upregulated, 550-fold from THP-1 to M1D0, and then had zero expression over the 12-day M1 culturing. Expression of TNFα was also significantly upregulated from THP-1 to M1D0 by 1100-fold, before having zero expression over the 12-day culturing period. Analysis of the data collected alludes to the fact that the macrophages in Sr^{2+} hydrogels could not help in promoting protein expression of M1 macrophages past the first day of M1 culturing.

For the Ca^{2+} crosslinked hydrogels, Figure 19, the expression of MCP-1 was significantly downregulated, 4-fold from THP-1 to M1D0, then further downregulated significantly over the 12-day culturing of Ca^{2+} crosslinked hydrogels. However, the expression of MCP-1 did not reach zero until day 12 of M1 culturing. IL1β expression was significantly upregulated, 750-fold from THP-1 to M1D0, and then downregulated on M1D3, before having zero expression over the remaining 12-day M1 culturing. Expression of TNFα was also significantly upregulated from THP-1 to M1D0 by 1.5-fold, before being downregulated from M1D0 to M1D3 by 4.25-fold, however, the

expression of TNFα did not reach zero until M1D9. Analysis of the data collected alludes to the fact that the macrophages in Ca^{2+} hydrogels maintained longer expression of M1 markers over the M1 culturing period than the Sr^{2+} crosslinked hydrogels. Results were analyzed using a comparative two-way ANOVA test, $p > 0.05$, with n=3.

3.5 The Impact of Sr^{2+} and Ca^{2+} Crosslinked Hydrogels' have on mRNA Expression of Macrophages

Reverse transcription-polymerase chain reaction was performed on hydrogel lysates (n=3) to measure the expression of select macrophage markers, namely ITGAM, Integrin Subunit Alpha M, (Marker for M0 adhesion), IL1β, Interleukin-1 beta, (M1 and an inflammatory cytokine marker) and CCR2, C-C chemokine receptor type 2, (Marker for M0 adhesion and inflammatory cytokine marker) were evaluated, Figures 14, 15, 16, and 17. For the Sr^{2+} crosslinked hydrogels there was no significant difference in the gene expression of ITGAM over the THP-1 monocytes to M0R macrophages culture duration of Sr^{2+} crosslinked hydrogels. However, we do see there is an increase in the expression of ITGAM from THP-1 to M0. The expression of inflammation cytokine marker, IL1β, was significantly enhanced 125-fold during the culturing of THP-1 cells to M0R cells. The expression of CCR2 is significantly downregulated 5-fold during the culturing of THP-1 cells to M0R cells. These results allude to the fact that Sr^{2+} is promoting the differentiation of THP-1 monocytes into M0 macrophages.

The mRNA gene expression of Ca^{2+} crosslinked hydrogels show a significant downregulation of ITGAM gene expression of M0R hydrogels during the culture duration of Ca^{2+} crosslinked hydrogels. The expression of inflammation cytokine marker, IL1β, was significantly enhanced 10-fold during the culturing of THP-1 cells to M0R

cells. The expression of CCR2 is significantly downregulated 12-fold during the culturing of THP-1 cells to M0 cells. Analysis of the data collected alludes to the fact that Ca^{2+} hydrogels did not promote M0 phenotype as well as Sr^{2+} crosslinked hydrogels over duration of M0R culture.

The mRNA expression of M1 gene markers were analyzed to determine how the ions impacted M1 phenotype differentiation. The gene expression of select macrophage markers, namely CD163 (Marker for M2 anti-inflammatory cytokine), IL1β (M1 and an inflammatory cytokine marker) and CD197 (Marker for M1) were evaluated by RTPCR. For the Sr^{2+} crosslinked hydrogels there was a significant upregulation of CD163 gene expression over the first 3 days of M1 development, followed by a significant downregulation on day 12 of M1 Sr^{2+} crosslinked hydrogels. The expression of inflammation cytokine marker, IL1β, was significantly enhanced 4-fold during the culturing of M1 macrophage cells. The expression of CD197 is significantly upregulated 28-fold during the culturing of M1 macrophage cells.

Analysis of Ca^{2+} crosslinked hydrogels showed a significant 3-fold upregulation of CD163 gene expression over the first 3 days of M1 development, followed by a non-significant downregulation on day 12 of M1 Ca^{2+} crosslinked hydrogels. The expression of inflammation cytokine marker, IL1β, was significantly enhanced during the culturing of M1 macrophage cells. The expression of CD197 is significantly upregulated 2.5-fold during the culturing of M1 macrophage cells. Analysis of the data collected alludes to the fact that Sr^{2+} hydrogels maintained the M1 phenotype over duration of culture more efficiently than the Ca^{2+} crosslinked hydrogel. Results were analyzed using a comparative one-way ANOVA test, $p > 0.05$, with $n=3$.

Chapter 4. Discussion and Future Work

It is proposed that with progressive disease of the joint that the synovial membrane thickens due to the excessive deposition of collagen–I. This leads to the stiffening of the basal synovial membrane. We hypothesize that the native cells of this membrane, namely macrophages and synovial fibroblasts may respond to this altered mechanical environment. In this thesis the effect of substrate stiffness on macrophage function and behavior was analyzed.

Previously reported literature [33] has evaluated the effect of substrate stiffness on polarization of bone marrow-derived macrophages (Raw264.7) by changing the percent concentration of acrylamide and bis-acrylamide solution in polyacrylamide hydrogels or the percent gelatin in gelatin-based. This study concluded that substrate stiffness had no impact on the proliferation of monocytes but did impact the polarization of macrophages. It was found that stiffer hydrogels promoted M2 macrophage phenotype, whereas the low stiffness hydrogels promoted M1 macrophage phenotype [33]. The study involving differing concentrations of gelatin (5-15%) found that macrophages would adopt an adhesive spreading morphology, and that the average spreading of cells across the hydrogel increased with increasing stiffness, concluding the findings that increasing substrate stiffness increases cell spreading [32]. This study followed up with analysis into the macrophages morphology and how it can be affected by the substrate stiffness. They concluded that softer hydrogels promoted elongated macrophages compared to the stiffer hydrogels. To conclude this experiment, they measured CD markers from the hydrogels and found that softer hydrogels promoted M1 macrophage polarization, and that hydrogels lead to lower protein secretion concentrations. Interestingly, another study

explored the utility of a copolymer of charge complementary heterodimeric coiled coil peptides and alginate as the polymer for hydrogel encapsulation of macrophages. This copolymer negated the use of conventional ionic crosslinking agents. In this study they found that the inflammation cytokines were significantly less expressed in the copolymer alginate compared to the Ca^{2+} crosslinked alginate. On account of the lower inflammatory expression, the study concluded that copolymerization was not a sufficient model for macrophage polarization [34]. In summary, the literature suggests that lower substrate stiffness promotes M1 macrophage polarization. However, none of these experiments tested the role of the crosslinking ion in macrophage polarization.

In a separate study, the impact of the valency of the crosslinking ion on the mechanical properties of the resultant alginate hydrogel was evaluated. In a comparison of Calcium, Strontium, and Barium ions crosslinking with alginate, Sr^{2+} ions were found to have a stronger binding affinity towards the G-blocks in alginate's structure, whereas Ca^{2+} had a stronger binding affinity towards the M-blocks [30]. Overall, the research showed that Ba^{2+} had the strongest affinity for alginate in totality, however, Ba^{2+} was found to create a hazardous environment within the hydrogels. The mechanical properties of alginate when crosslinked with Ca^{2+} or Sr^{2+} showed to be equally comparable. Based on this published report, it is our assertion that Sr^{2+} and Ca^{2+} ions would be optimal variables for testing the effects of crosslinking ions with alginate on macrophage polarization. Hence in this research we have employed crosslinking via Sr^{2+} and Ca^{2+} to change the substrate stiffness.

The mechanical analysis of the Sr^{2+} and Ca^{2+} crosslinked hydrogels show that pores develop in M1 cultured hydrogels, but not in monocyte or cell-less hydrogels. In addition,

the average pore size of the Ca^{2+} crosslinked hydrogels were slightly larger than the Sr^{2+} crosslinked hydrogels, but these results were not significant. When comparing the rheological measurements of the hydrogels Ca^{2+} crosslinked hydrogels showed to increase in G' pressure over the culturing, indicating that the Ca^{2+} were still crosslinking with alginate over time. The Sr^{2+} crosslinked hydrogels however, maintained a consistent G' over the 14-day period, suggesting that Sr^{2+} quickly reached full crosslinking and maintained it. The G' measurements allow for the comparison of the hydrogels' retention to deformation, how structurally stable are the hydrogels. The G" data provide information on the fluidness of the hydrogels. The G" of the two hydrogels indicates no significant difference. Both ions provided strong crosslinking with the alginate, preventing structural instability.

We looked at the viability of macrophages in the hydrogels, as M1 macrophages are known for their short survival time. The live/dead analysis of macrophage characterization indicated that Sr^{2+} crosslinked hydrogels were able to maintain cellular viability in M1 culturing more efficiently than Ca^{2+} crosslinked hydrogels. The data show that Sr^{2+} crosslinked hydrogels maintained a higher viability of macrophage cells (M1), 85.32%, than the Ca^{2+} crosslinked hydrogels did, 67.50%. Nevertheless, the ELISA data indicate that Ca^{2+} crosslinked hydrogels prolonged the expression of M1 protein concentrations further into culturing than the Sr^{2+} crosslinked hydrogels. Contradictory to this, the rt-PCR data suggest that Sr^{2+} crosslinked hydrogels promoted M0 and M1 RNA expression to a greater magnitude throughout culturing.

Providing a more in-depth understanding of how ions interact with macrophages within a hydrogel environment will help provide more insight into target treatment

designs for joint diseases, such as osteoarthritis (OA), rheumatoid arthritis (RA), or psoriatic arthritis (PsA). Promotion of macrophage polarization and healing within these harsh and stiffen environments has been a struggle in the biomedical field, leading to millions of people suffering with these arthritic conditions.

In summary, the hydrogels with Sr^{2+} as the crosslinking agent promoted a more stable crosslink of the alginate hydrogel and provided a more suitable environment for M1 polarization. The limitation of this study, however, is the use of only one concentration of ions and using only blood derived monocyte (THP-1), and not a second blood-derived macrophages. With these variables implemented into the study we could test how the ions impact macrophage polarization through differing stiffnesses of alginate. In addition, the use of THP-1 cells only does not provide an accurate representation of how all monocytes will proliferate and attach within a hydrogel.

Future steps in this project include implementing more concentrations of ions to provide a more in-depth understanding of the ion's impact on macrophage development. Additionally, various monocyte cell lines would be explored to determine if the results are consistent across monocytes, or if the findings were specific to the THP-1 cell-line.

References

[1] P. J. Cope, K. Ourradi, Y. Li, and M. Sharif, "Models of osteoarthritis: the good, the bad and the promising," *Osteoarthritis Cartilage*, vol. 27, no. 2, p. 230, Feb. 2019, doi: 10.1016/J.JOCA.2018.09.016.

[2] P. Juneja, A. Munjal, and J. B. Hubbard, "Anatomy, Joints," *StatPearls*, Apr. 2023, Accessed: Aug. 28, 2023. [Online]. Available: https://www.ncbi.nlm.nih.gov/books/NBK507893/

[3] H. Long *et al.*, "Prevalence Trends of Site-Specific Osteoarthritis From 1990 to 2019: Findings From the Global Burden of Disease Study 2019," *Arthritis and Rheumatology*, vol. 74, no. 7, pp. 1172–1183, Jul. 2022, doi: 10.1002

[4] T. M. Tamer, "Hyaluronan and synovial joint: Function, distribution and healing," *Interdiscip Toxicol*, vol. 6, no. 3, pp. 111–125, Sep. 2013, doi: 10.2478/INTOX-2013-0019.

[5] J. A. Buckwalter, D. D. Anderson, T. D. Brown, Y. Tochigi, and J. A. Martin, "The Roles of Mechanical Stresses in the Pathogenesis of Osteoarthritis: Implications for Treatment of Joint Injuries," *SageJournals*, vol. 4, no. 4, pp. 286–294, Oct. 2013, doi: 10.1177/1947603513495889.

[6] U. Nedunchezhiyan, I. Varughese, A. R. J. Sun, X. Wu, R. Crawford, and I. Prasadam, "Obesity, Inflammation, and Immune System in Osteoarthritis," *Frontiers in Immunology*, vol. 13. Frontiers Media S.A., Jul. 04, 2022. doi: 10.3389/fimmu.2022.907750.

[7] R. F. Loeser, “Aging processes and the development of osteoarthritis,” *Curr Opin Rheumatol*, vol. 25, no. 1, pp. 108–113, Jan. 2013, doi: 10.1097/BOR.0B013E32835A9428.

[8] E. Sanchez-Lopez, R. Coras, A. Torres, N. E. Lane, and M. Guma, “Synovial inflammation in osteoarthritis progression,” *Nature Reviews Rheumatology 2022 18:5*, vol. 18, no. 5, pp. 258–275, Feb. 2022, doi: 10.1038/s41584-022-00749-9.

[9] P. Alarcon *et al.*, “Metabolic disturbances in synovial fluid are involved in the onset of synovitis in heifers with acute ruminal acidosis”, doi: 10.1038/s41598-019-42007-1.

[10] C. N. Tran, S. K. Lundy, and D. A. Fox, “Synovial biology and T cells in rheumatoid arthritis,” *Pathophysiology*, vol. 12, pp. 183–189, 2005, doi: 10.1016/j.pathophys.2005.07.005.

[11] A. Kennedy, U. Fearon, D. J. Veale, C. Godson, F. Saverio, and D. Giovine, “Macrophages in synovial inflammation,” 2011, doi: 10.3389/fimmu.2011.00052.

[12] P. J. Murray *et al.*, “Macrophage Activation and Polarization: Nomenclature and Experimental Guidelines,” *Immunity*, vol. 41, no. 1, pp. 14–20, Jul. 2014, doi: 10.1016/J.IMMUNI.2014.06.008.

[13] C. Bogdan, “Nitric oxide and the immune response. - EBSCO,” Nature Publishing Group. Accessed: Aug. 11, 2023. [Online]. Available: https://research-ebsco-com.elib.uah.edu/c/ip4evp

[14] D. M. Mosser and J. P. Edwards, “Exploring the full spectrum of macrophage activation,” *Nat Rev Immunol*, vol. 8, no. 12, pp. 958–969, Dec. 2008, doi: 10.1038/NRI2448.

[15] S. Gordon and P. R. Taylor, “Monocyte and macrophage heterogeneity,” *Nat Rev Immunol*, vol. 5, no. 12, pp. 953–964, Dec. 2005, doi: 10.1038/NRI1733.

[16] Y. Lavin *et al.*, “Tissue-Resident Macrophage Enhancer Landscapes Are Shaped by the Local Microenvironment,” *Cell*, vol. 159, no. 6, pp. 1312–1326, Dec. 2014, doi: 10.1016/J.CELL.2014.11.018.

[17] P. Krzyszczyk, R. Schloss, A. Palmer, and F. Berthiaume, “The Role of Macrophages in Acute and Chronic Wound Healing and Interventions to Promote Pro-wound Healing Phenotypes,” *Front Physiol*, vol. 9, no. MAY, p. 419, May 2018, doi: 10.3389/FPHYS.2018.00419.

[18] F. Geissmann, S. Jung, and D. R. Littman, “Blood Monocytes Consist of Two Principal Subsets with Distinct Migratory Properties,” *Immunity*, vol. 19, no. 1, pp. 71–82, Jul. 2003, doi: 10.1016/S1074-7613(03)00174-2.

[19] L. Bosurgi *et al.*, “Macrophage function in tissue repair and remodeling requires IL-4 or IL-13 with apoptotic cells,” *Science (1979)*, vol. 356, no. 6342, pp. 1072–1076, 2017, [Online]. Available: https://www-jstor-org.elib.uah.edu/stable/26399200

[20] L. Ziegler-Heitbrock *et al.*, “Nomenclature of monocytes and dendritic cells in blood,” *Blood*, vol. 116, no. 16, pp. e74–e80, Oct. 2010, doi: 10.1182/BLOOD-2010-02-258558.

[21] I. Kwiecień, M. Polubiec-Kownacka, D. Dziedzic, D. Wołosz, P. Rzepecki, and J. Domagała-Kulawik, “CD163 and CCR7 as markers for macrophage polarization in lung cancer microenvironment,” *Cent Eur J Immunol*, vol. 44, no. 4, p. 395, 2019, doi: 10.5114/CEJI.2019.92795.

[22] C. Rodrigues Nascimento, N. Ap, R. Fernandes, L. Andrea Gonzalez Maldonado, and C. Rossa Junior, "Comparison of monocytic cell lines U937 and THP-1 as macrophage models for in vitro studies," 2022, doi: 10.1016/j.bbrep.2022.101383.

[23] M. A. Ingersoll *et al.*, "Comparison of gene expression profiles between human and mouse monocyte subsets," *Blood*, vol. 115, no. 3, pp. e10–e19, Jan. 2010, doi: 10.1182/BLOOD-2009-07-235028.

[24] H. Geckil, F. Xu, X. Zhang, S. Moon, and U. Demirci, "Engineering hydrogels as extracellular matrix mimics," *Nanomedicine (Lond)*, vol. 5, no. 3, p. 469, Apr. 2010, doi: 10.2217/NNM.10.12.

[25] L. S. Saleh, M. Carles-Carner, and S. J. Bryant, "The in vitro effects of macrophages on the osteogenic capabilities of MC3T3-E1 cells encapsulated in a biomimetic poly(ethylene glycol) hydrogel," *Acta Biomater*, vol. 71, p. 37, Apr. 2018, doi: 10.1016/J.ACTBIO.2018.02.026.

[26] S. N. King, S. E. Hanson, X. Chen, J. Kim, P. Hematti, and S. L. Thibeault, "In vitro characterization of macrophage interaction with mesenchymal stromal cell – hyaluronan hydrogel constructs," *J Biomed Mater Res A*, vol. 102, no. 3, p. 890, Mar. 2014, doi: 10.1002/JBM.A.34746.

[27] Y. Liang and K. L. Kiick, "Heparin-functionalized polymeric biomaterials in tissue engineering and drug delivery applications," *Acta Biomater*, vol. 10, no. 4, pp. 1588–1600, Apr. 2014, doi: 10.1016/J.ACTBIO.2013.07.031.

[28] G. T. Grant, E. R. Morris, D. A. Rees, P. J. C. Smith, and D. Thom, "Biological interactions between polysaccharides and divalent cations: The egg-box model,"

FEBS Lett, vol. 32, no. 1, pp. 195–198, May 1973, doi: 10.1016/0014-5793(73)80770-7.

[29] W. R. Gombotz and S. F. Wee, "Protein release from alginate matrices," *Adv Drug Deliv Rev*, vol. 31, no. 3, pp. 267–285, May 1998, doi: 10.1016/S0169-409X(97)00124-5.

[30] Ý. A. Mørch, I. Donati, B. L. Strand, and G. Skjåk-Bræk, "Effect of Ca2+, Ba2+, and Sr2+ on alginate microbeads," *Biomacromolecules*, vol. 7, no. 5, pp. 1471–1480, May 2006, doi: 10.1021/BM060010D

[31] X. Zhang, L. Wang, L. Weng, and B. Deng, "Strontium ion substituted alginate-based hydrogel fibers and its coordination binding model," *J Appl Polym Sci*, vol. 137, no. 16, p. 48571, Apr. 2020, doi: 10.1002/APP.48571.

[32] Z. Zhuang *et al.*, "Control of Matrix Stiffness Using Methacrylate-Gelatin Hydrogels for a Macrophage-Mediated Inflammatory Response," *ACS Biomater Sci Eng*, vol. 6, no. 5, pp. 3091–3102, May 2020, doi: 10.1021/ACSBIOMATERIALS.0C00295

[33] M. Chen *et al.*, "Substrate stiffness modulates bone marrow-derived macrophage polarization through NF-κB signaling pathway," *Bioact Mater*, vol. 5, no. 4, p. 880, Dec. 2020, doi: 10.1016/J.BIOACTMAT.2020.05.004.

[34] Z. Clapacs *et al.*, "Coiled Coil Crosslinked Alginate Hydrogels Dampen Macrophage-Driven Inflammation," *Biomacromolecules*, vol. 23, no. 3, pp. 1183–1194, Mar. 2022, doi: 10.1021/ACS.BIOMAC.1C01462

Figures

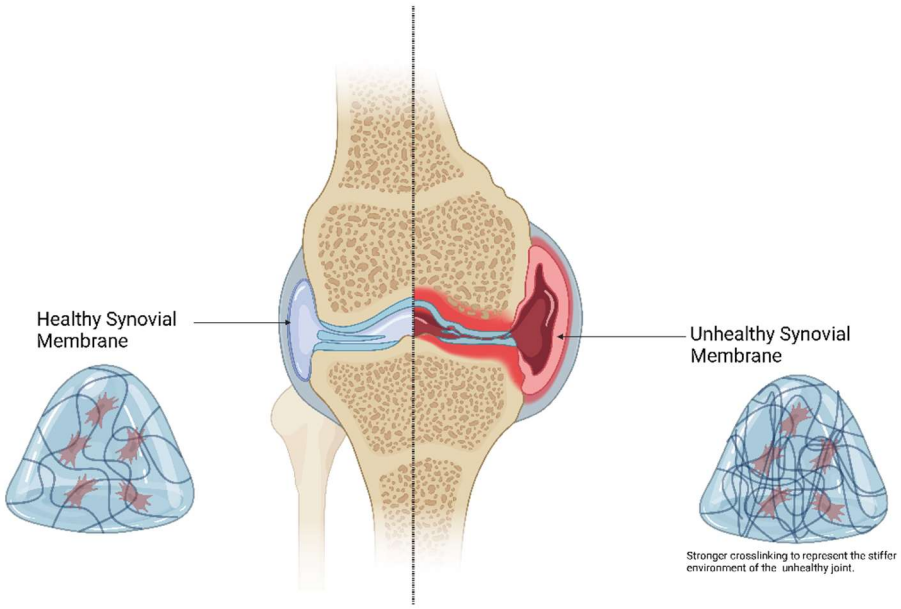

Figure 1 Diagram illustrating a knee joint with a health versus unhealthy synovium. Diagram illustrating a knee joint with a health versus unhealthy synovium, and how the conditions are recreated in a hydrogel.

Figure 2 Image of THP-1 cells in RPMI media. Image of THP-1 cells in RPMI media taken using an inverted light microscope at 4x.

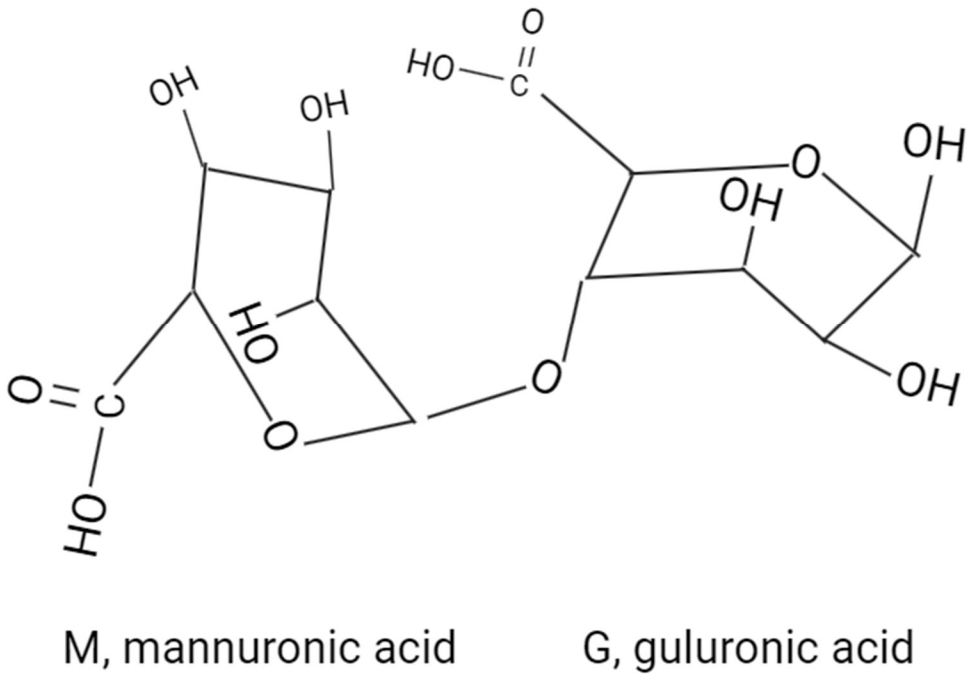

Figure 3 An illustration of alginate M:G block binding.

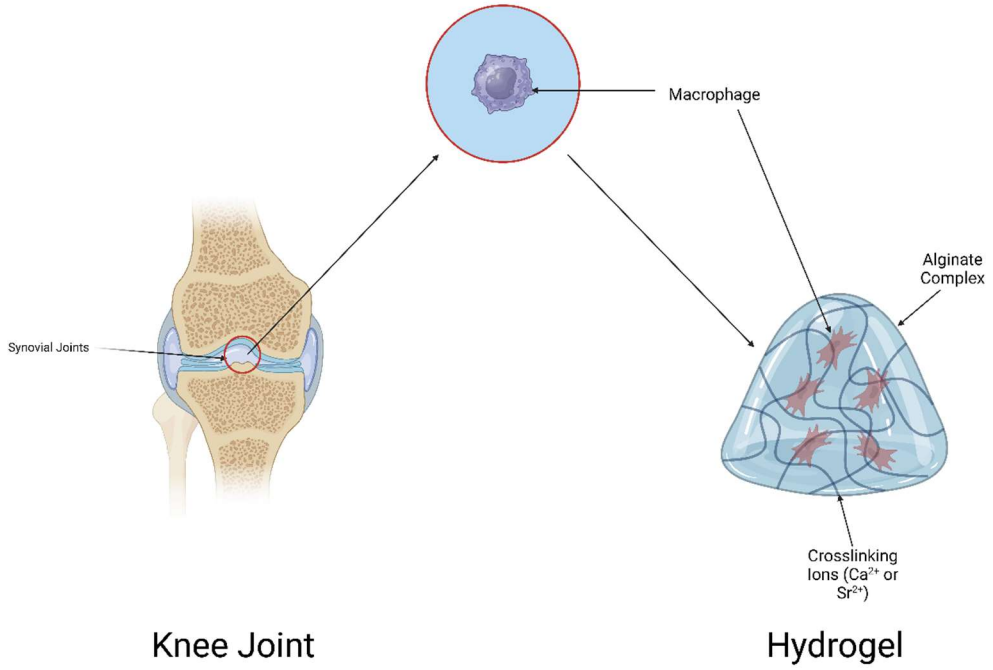

Figure 4 An illustration of how hydrogels mimic the environment of the synovium with the seeding of macrophages.

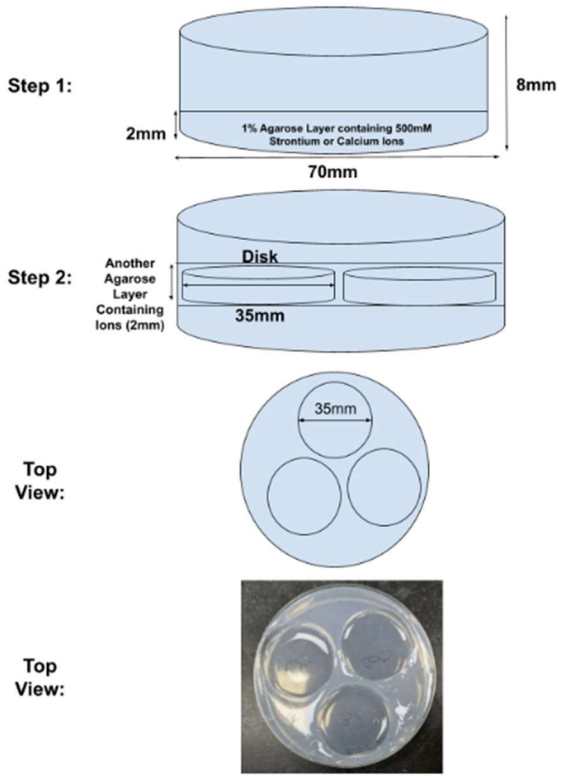

Figure 5 Schematic for Rheological Hydrogel Testing. A mechanism for pouring the agarose plate for rheological measurements, including both a side and top-down view of the wells.

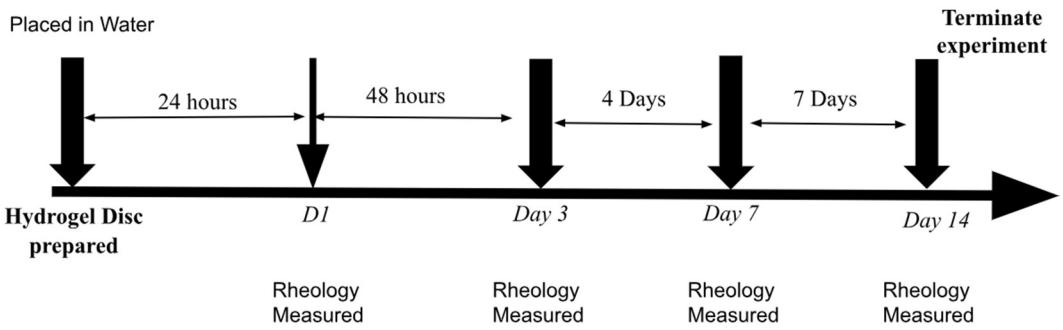

Figure 6 Schematic for Rheological Hydrogel Testing. Timeline of rheological data analysis and hydrogel culturing.

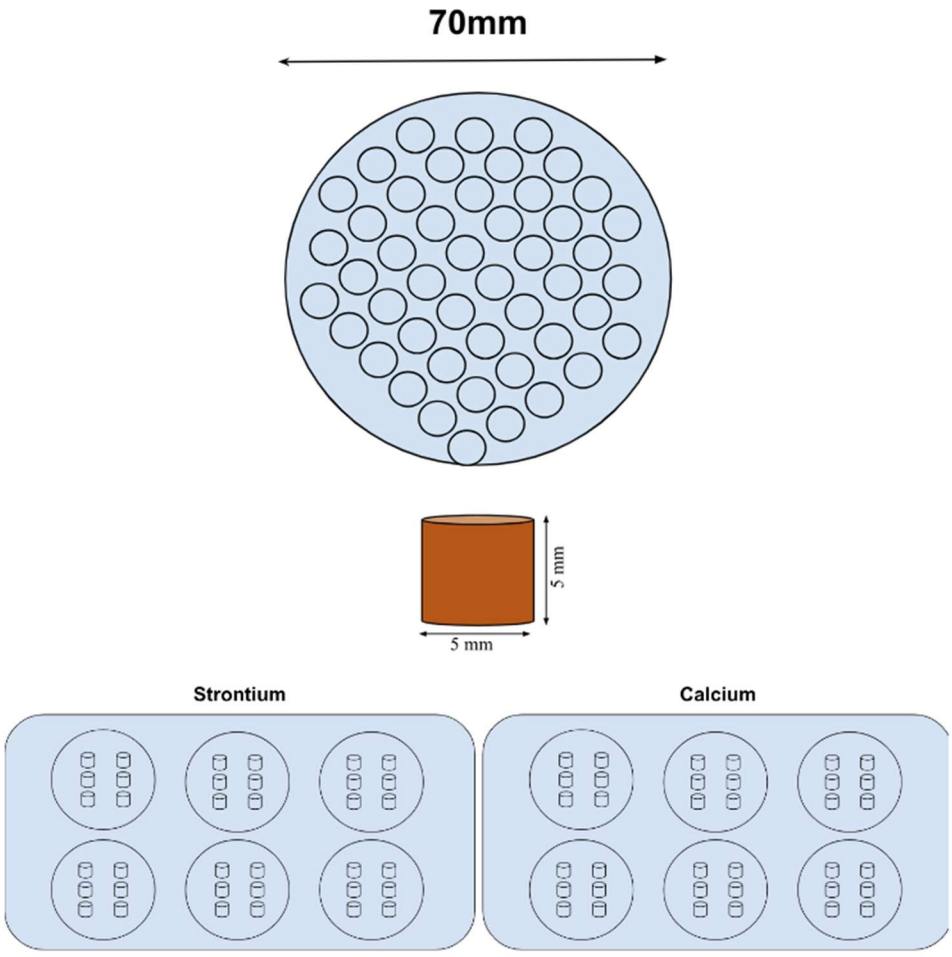

Figure 7 Schematic for Hydrogel Encapsulated Cell Culturing. Schematics for hydrogel encapsulation of cells.

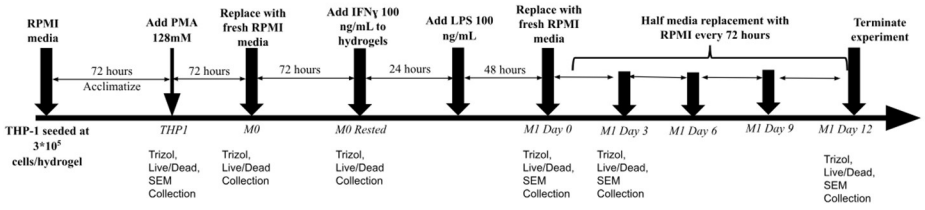

Figure 8 Schematic for Hydrogel Encapsulated Cell Culturing. Timeline of hydrogel encapsulated monocyte and macrophage cell culturing.

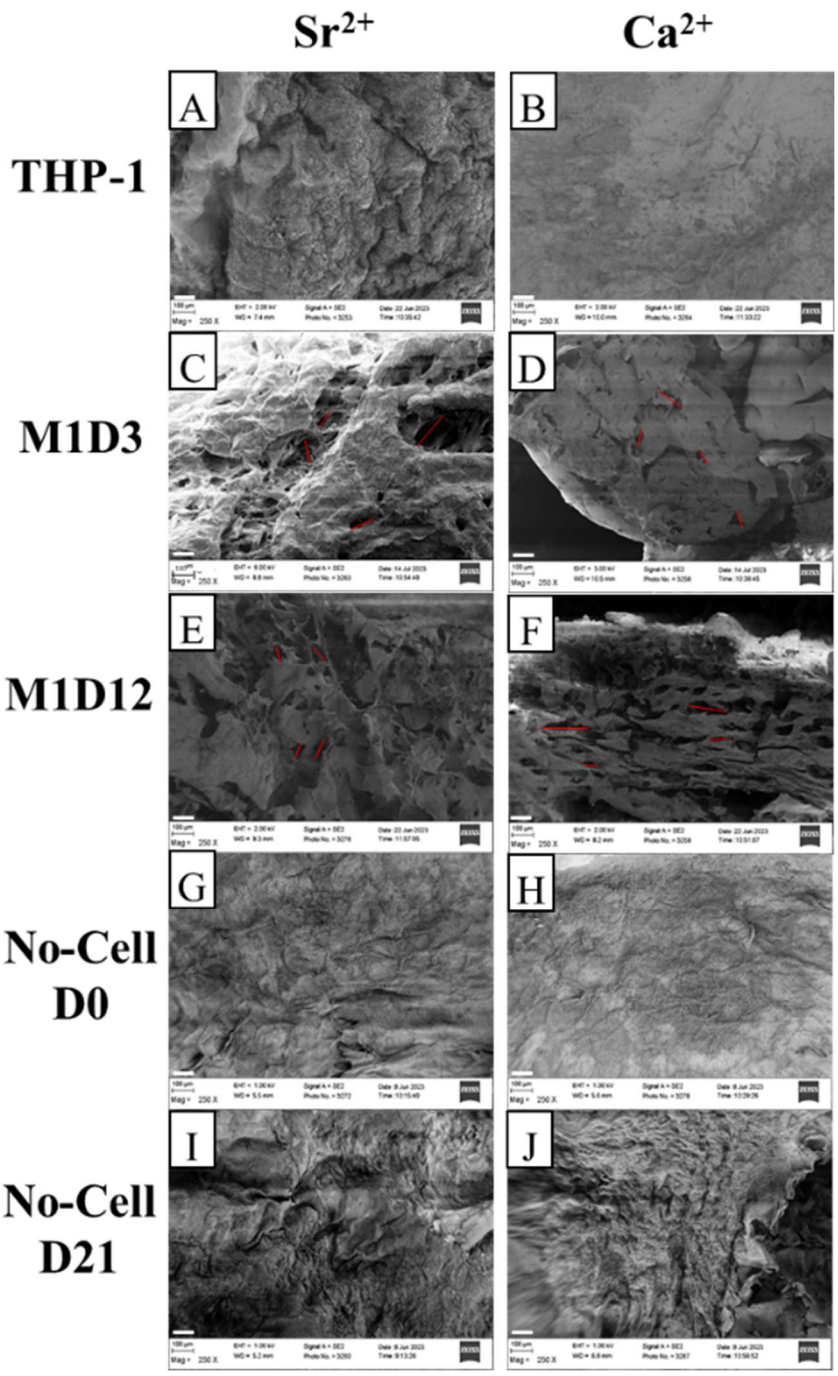

Figure 9 Hydrogel Pore Analysis. Scanning electron microscope images of hydrogel surface. A) Sr^{2+} crosslinked hydrogel encapsulated THP-1 cells, B) Ca^{2+} crosslinked hydrogel encapsulated THP-1 cells, C) Sr^{2+} crosslinked hydrogel encapsulated M1D3 cells, D) Ca^{2+} crosslinked hydrogel encapsulated M1D3 cells, E) Sr^{2+} crosslinked hydrogel encapsulated M1D12 cells, F) Ca^{2+} crosslinked hydrogel encapsulated M1D12 cells, G) No-cell Day1 Sr^{2+} crosslinked hydrogels, H) No-cell Day1 Ca^{2+} crosslinked hydrogels, I) No-cell Day21 Sr^{2+} crosslinked hydrogels, J) No-cell Day21 Ca^{2+} crosslinked hydrogels.

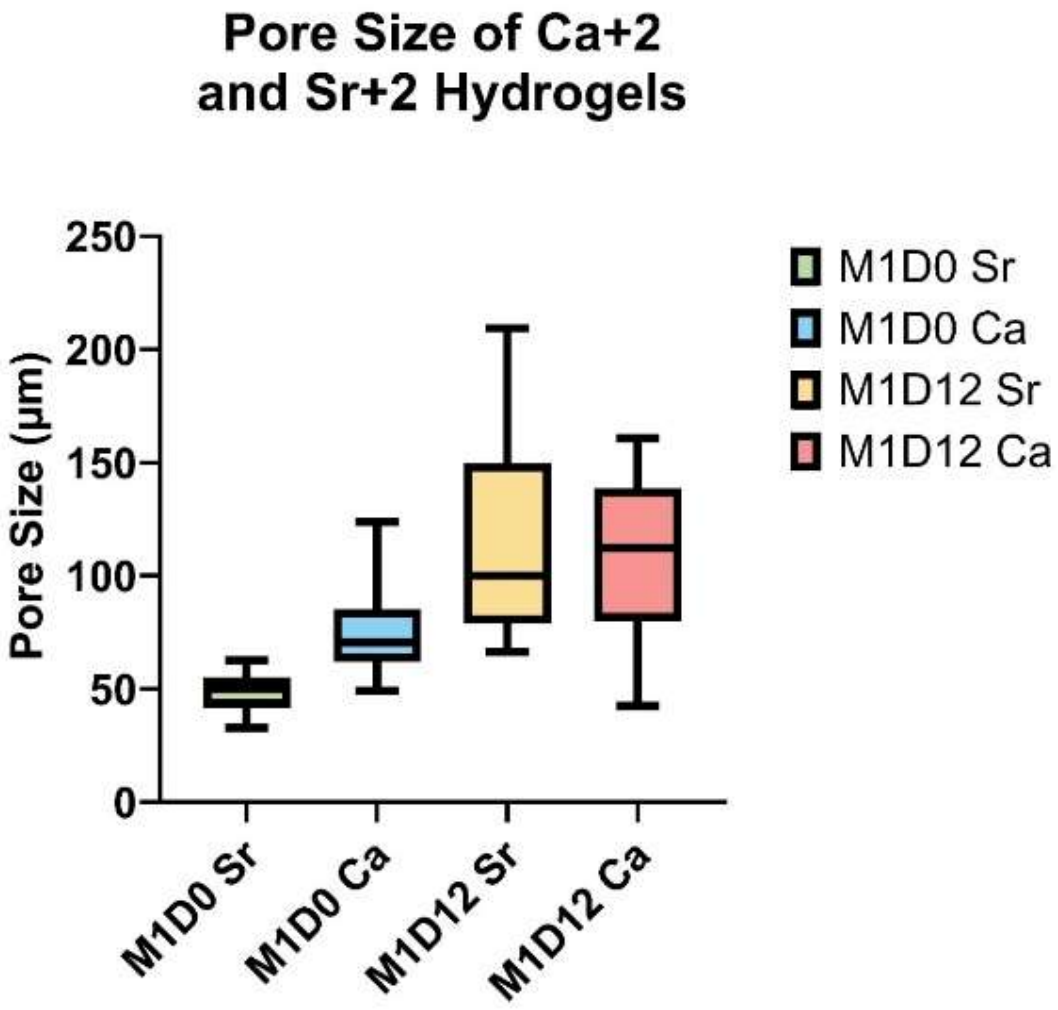

Figure 10 Hydrogel Pore Analysis. The surface pore diameter measurements from the images taken using scanning electron microscope and analyzed using ImageJ™. Pores, 27, were measured as n=3. Hydrogels before M1 development and hydrogels without cells did not contain any pores. Data were analyzed using a two-way ANOVA comparison test, with $p < 0.005$.

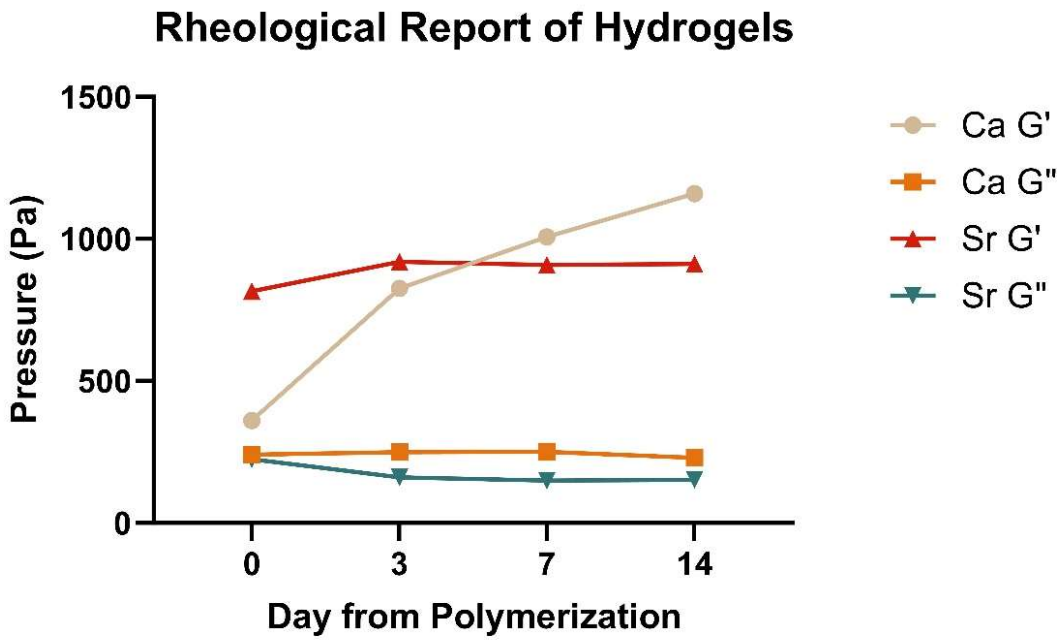

Figure 11 Rheological Analysis. The rheological measurements of G' and G" from hydrogels across 14 days. The data represent the average pressure (n=3) with each hydrogel being measured 20 times. Data were analyzed using a two-way ANOVA comparison test, with $p < 0.005$.

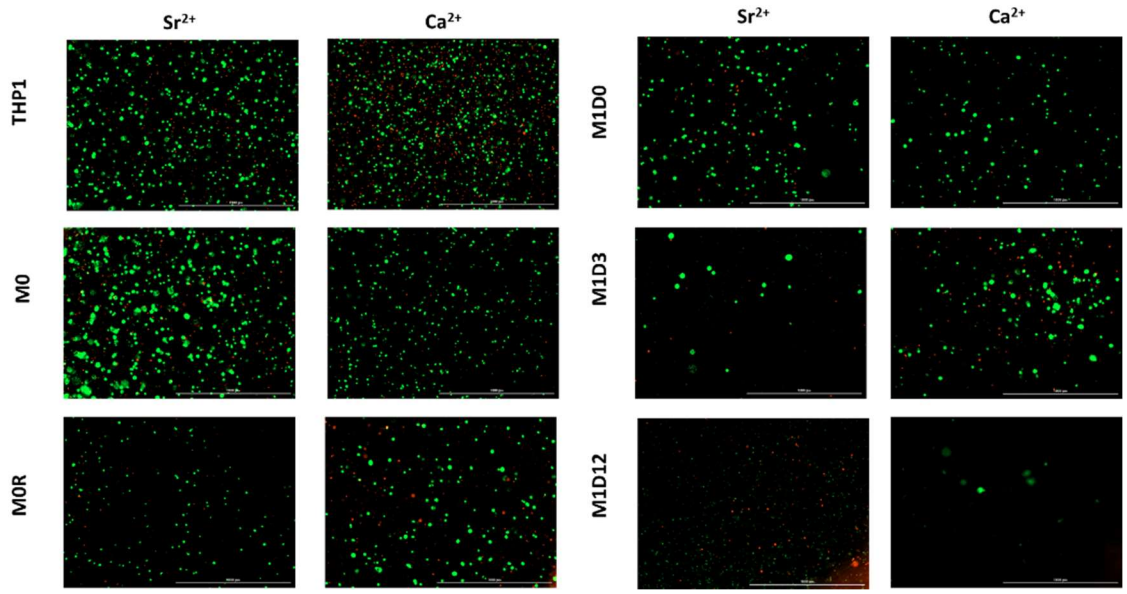

Figure 12 Live/Dead Analysis. Representative Live/Dead images taken with a fluorescence microscope at 20x.

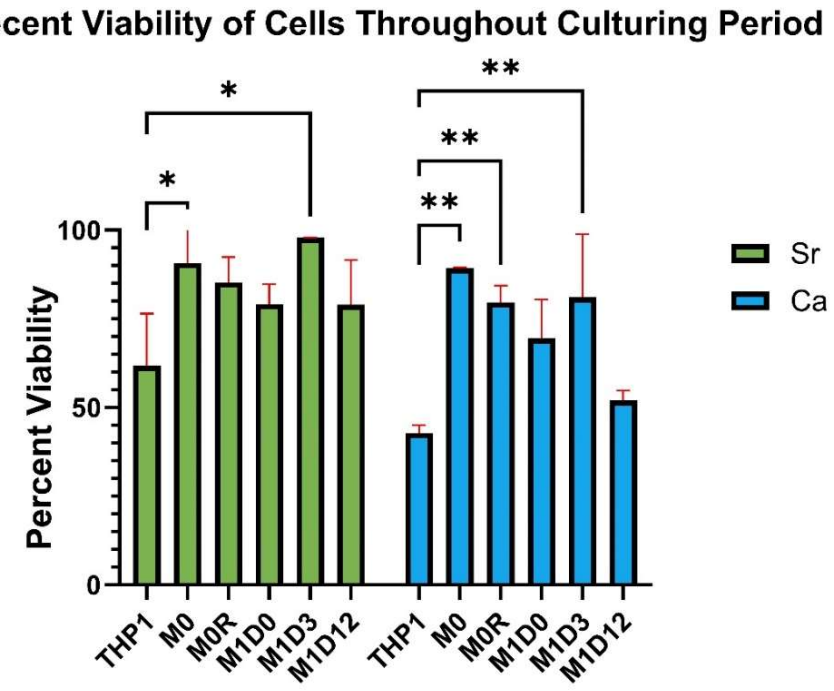

Figure 13 Live/Dead Analysis. The precent viability of Sr^{2+} and Ca^{2+} crosslinked hydrogel encapsulated across total culture. Results represent the average percent of live cells to total cells in a hydrogel ± standard error (n=2). Data were analyzed using a two-way ANOVA caparison test, ns represents non-significant, * represents p value >0.01, ** represents p value <0.01, *** represents p value <0.001 and **** represents p value <0.0001.

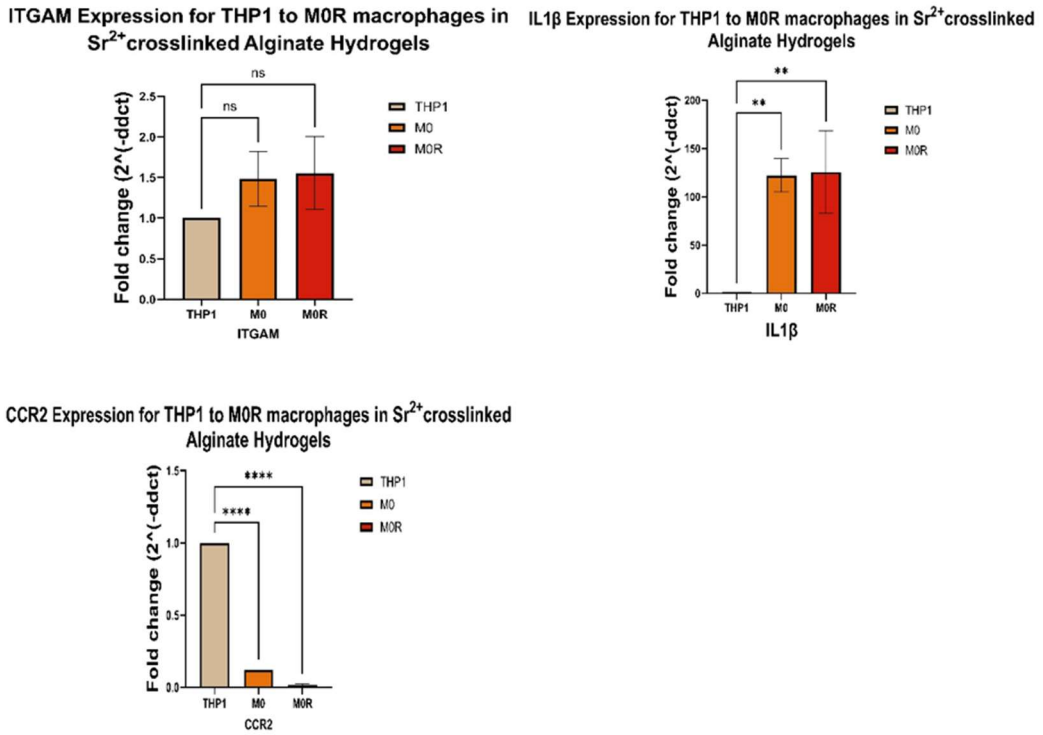

Figure 14 Reverse Transcription Polymerase Chain Reaction (RT-PCR) Analysis. The mRNA expression of ITGAM, IL1β, and CCR2 from Sr^{2+} crosslinked hydrogels from monocyte to M0R culturing measured by RT-PCR. The data represent the average concentration ± standard error (n=3). Results were analyzed using a comparative two-way ANOVA comparison test, ns represents non-significant, * represents p value >0.01, ** represents p value <0.01, *** represents p value <0.001 and **** represents p value <0.0001.

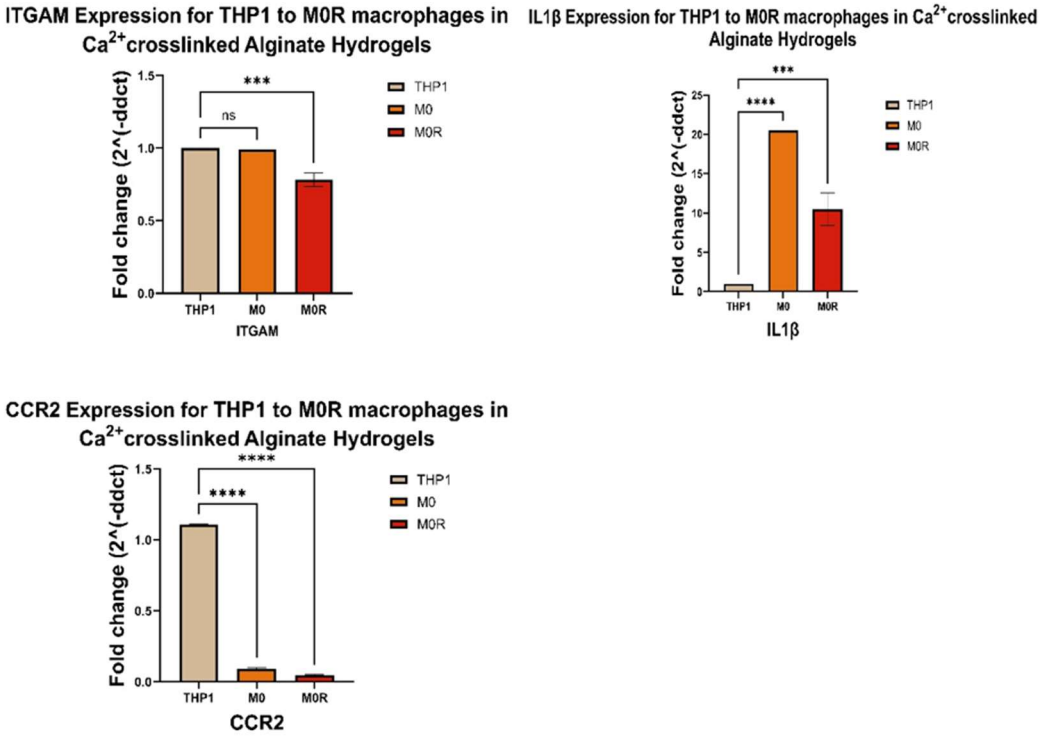

Figure 15 Reverse Transcription Polymerase Chain Reaction (RT-PCR) Analysis. The mRNA expression of ITGAM, IL1β, and CCR2 from Ca^{2+} crosslinked hydrogels from monocyte to M0R culturing measured by RT-PCR. The data represent the average concentration ± standard error (n=3). Results were analyzed using a comparative two-way ANOVA comparison test, ns represents non-significant, * represents p value >0.01, ** represents p value <0.01, *** represents p value <0.001 and **** represents p value <0.0001.

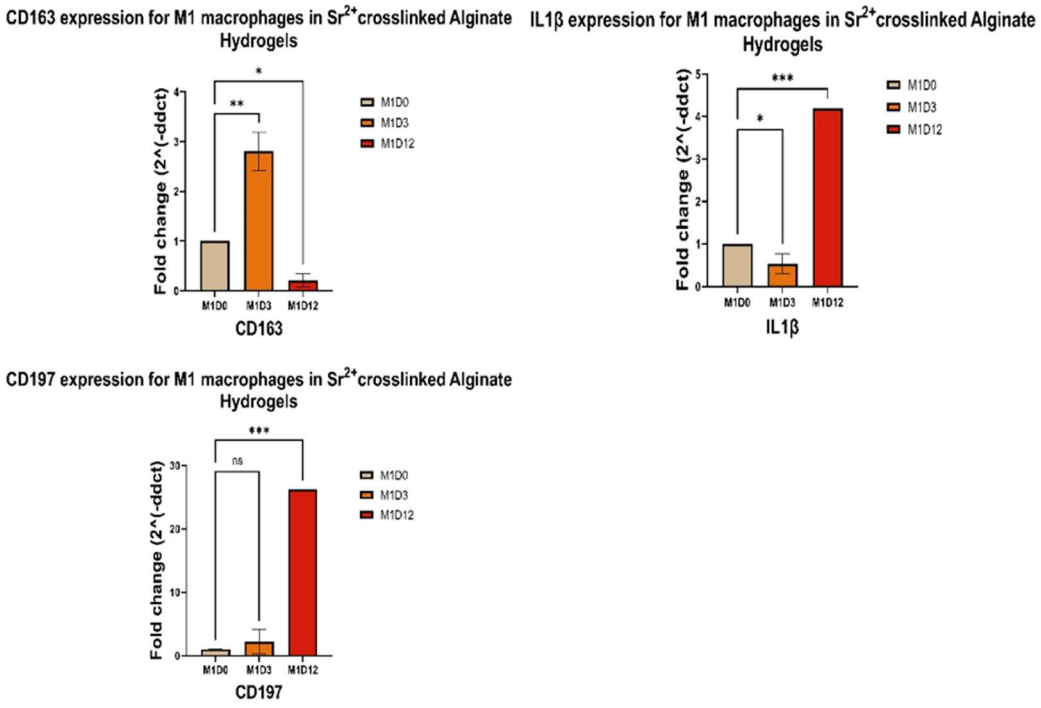

Figure 16 Reverse Transcription Polymerase Chain Reaction (RT-PCR) Analysis. The mRNA expression of CD163, IL1β, and CD197 from Sr^{2+} crosslinked hydrogels from M1 culturing measured by RT-PCR. The data represent the average concentration ± standard error (n=3). Results were analyzed using a comparative two-way ANOVA comparison test, ns represents non-significant, * represents p value >0.01, ** represents p value <0.01, *** represents p value <0.001 and **** represents p value <0.0001.

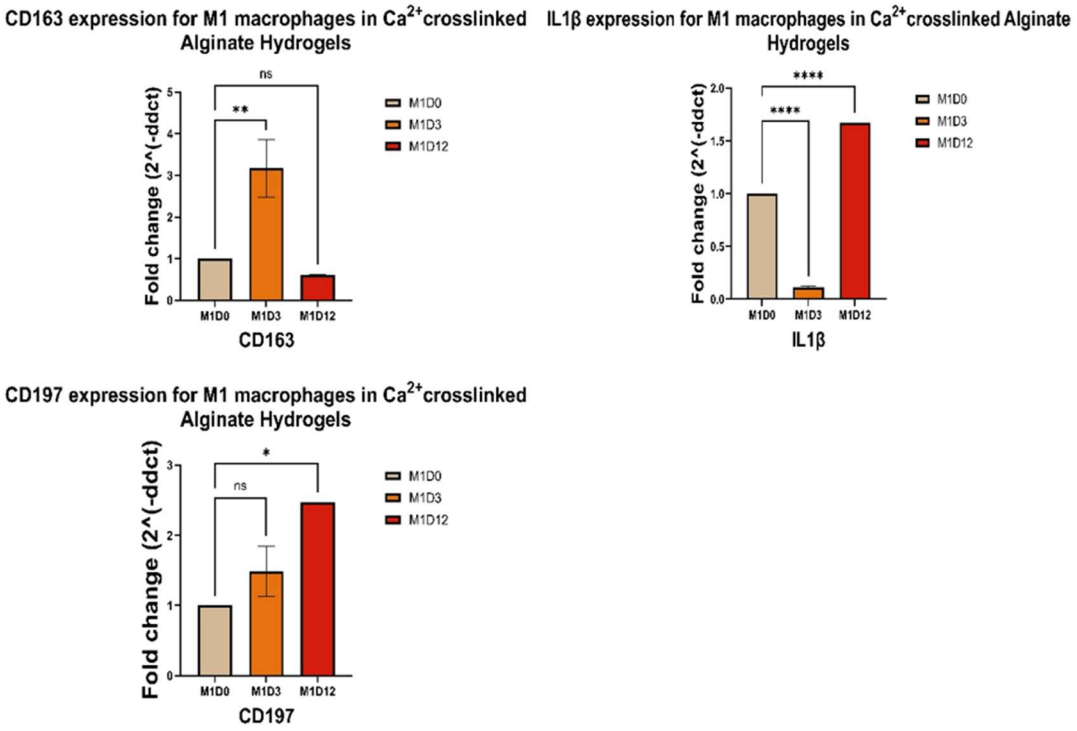

Figure 17 Reverse Transcription Polymerase Chain Reaction (RT-PCR) Analysis. The mRNA expression of CD163, IL1β, and CD197 from Ca^{2+} crosslinked hydrogels from M1 culturing measured by RT-PCR. The data represent the average concentration ± standard error (n=3). Results were analyzed using a comparative two-way ANOVA comparison test, ns represents non-significant, * represents p value >0.01, ** represents p value <0.01, *** represents p value <0.001 and **** represents p value <0.0001.

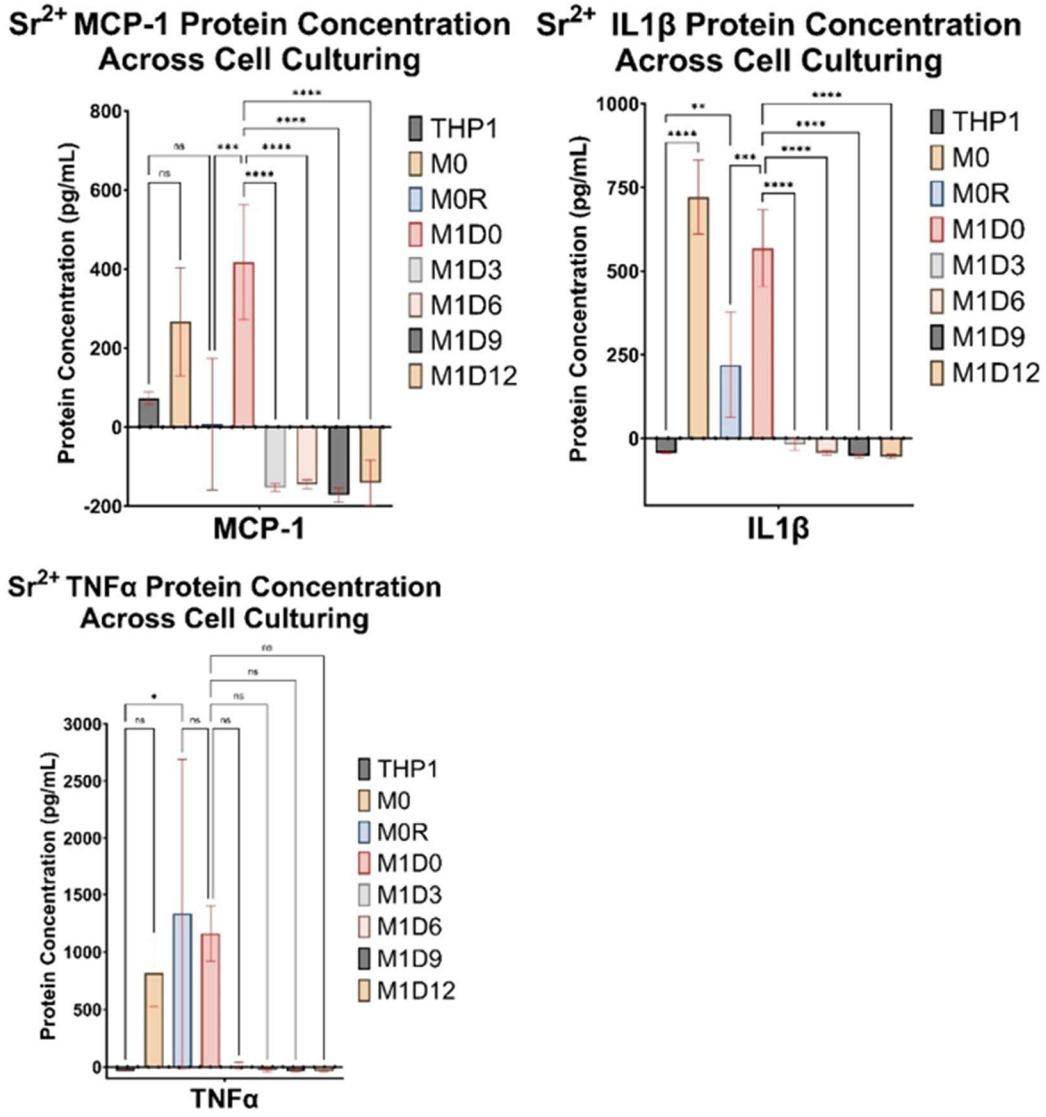

Figure 18 Enzyme-Linked Immunoassay (ELISA) Analysis. The protein concentration of MCP-1, IL1β, and TNFα from Sr^{2+} crosslinked hydrogels throughout the total culture measured by ELISA. The data represent the average concentration ± standard error (n=3). Results were analyzed using a comparative two-way ANOVA comparison test, ns represents non-significant, * represents p value >0.01, ** represents p value <0.01, *** represents p value <0.001 and **** represents p value <0.0001.

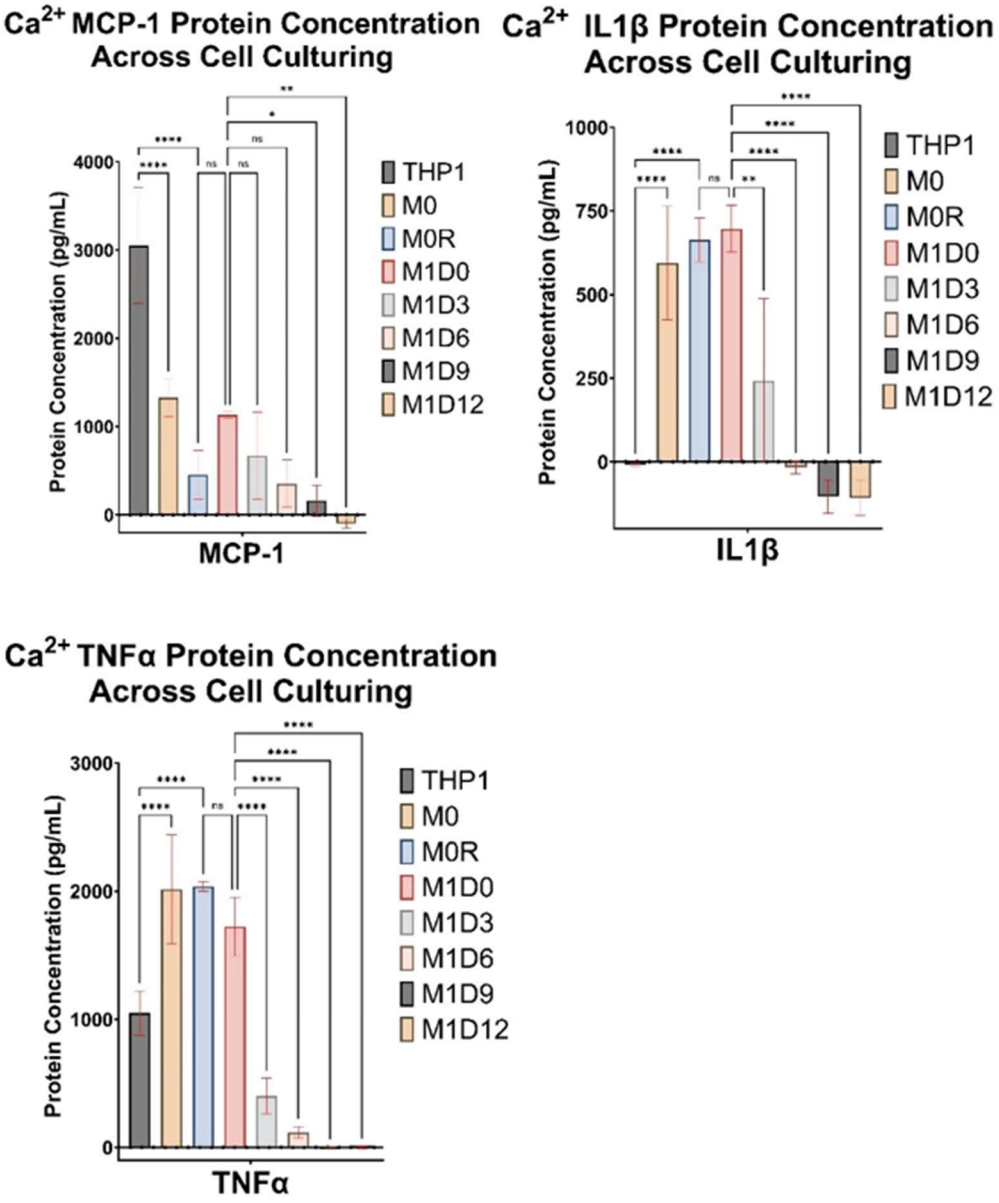

Figure 19 Enzyme-Linked Immunoassay (ELISA) Analysis. The protein concentration of MCP-1, IL1β, and TNFα from Ca^{2+} crosslinked hydrogels throughout the total culture measured by ELISA. The data represent the average concentration ± standard error (n=3). Results were analyzed using a comparative two-way ANOVA comparison test, ns represents non-significant, * represents p value >0.01, ** represents p value <0.01, *** represents p value <0.001 and **** represents p value <0.0001.

Tables

Table 1: Preparation of RT PCR mix for Real time PCR.

Component (Life Technologies Gene Expression Assays)	**Volume for one reaction /one well**
TaqMan® RT-PCR Mix (2✕)	5.0 µL
TaqMan® Gene Expression Assay (20✕)	0.5 µL
Taq Man®RT Enzyme Mix (40✕)	0.25 µL
RNA sample (50 ng/µL)	x µL
RNase free water	(10 – x) µL
Total volume /well	10 µl

Table 2: Thermal cycling conditions for Real time PCR.

Stage	Step	Temperature (ºC)	Time
Holding	Reverse transcription	48	15min
Holding	Activation of AmpliTaq Gold® DNA Polymerase, Ultra-Pure	95	10min
Cycling (40 cycles)	Denature	95	15 sec
	Anneal/extend	60	1 min

Table 3: List of primers used.

GAPDH	**Thermo Scientific**	**Hs02786624_g1**	**1861108**
CCR2	Thermo Scientific	Hs00704702_s1	1836679
ITGAM	Thermo Scientific	Hs00167204_m1	1815367
CCR7	Thermo Scientific	Hs01013469_m1	2020942
CD163	Thermo Scientific	Hs00174705_m1	1869600

Appendix A. Materials

Table A.1 Equipment Used. List of all equipment used throughout the experiment, including the vendor, model number, and serial number, if applicable.

Item	Vendor	Model #	Serial #
Incubator	Bel-Art Products	420741118	6183001
SEM Machine	Zeiss	LEO 1550	2004
Centrifuge	Eppendorf	5424	5424BK845322
Centrifuge	Eppendorf	5425	5405LH723647
Microwave	Emerson	MW8871W	71001051GG
Mass Scale	Denver Instrument	P-4002	P4K2052005
Inverted Microscope	Fisherbrand	03000013	20190101367
4℃ Refrigerator	Fisherbrand	1163511401191113	20LFEEFSA
-20℃ White Refrigerator	VWR	SCPAF-3020	SYM-14G0378-1408
-80℃ Grey Refrigerator	DW-86L486	BE0EZ9E1T00B2CCT0007	VWR
Lionheart Automated Fluorescence Microscope	BioTek Instruments	1908078	LLX
Vortex-Genie 2	Scientific Industries	2-336926	G-560

Quant Studio 3 RNA reading machine	Applied Biosystem	IEC61326	272312373
Microplate reader	BioTek	800TS	1901090
Automated Cell Counter	Bio-Rad	508BR03226	TC20
pH meter	Orion Star	A211	X45380
Magnetic Stirrer	Fisher Scientific	120S	206N0835
Autoclave	Tuttnauer	3870RLP-B/L-D	18051804
Nanodrop	Thermo Scientific	ONEc	AZY1811912
Incubator	Eppendorf	C170i	6731JL407967
Water Bath	Corning	LSE	17070562

Table A.2 Software's Used. List of all software used throughout the experiment, including the procedure it was used in, the software, and the edition, if applicable.

Procedure	Software	Edition
Microscope	Gen5	3.13
Image Analysis	ImageJ™	1.53t Java
Rheometer	HAAKE RheoWin	N/A
SEM	SmartSEM	5.07

Table A.3 Hydrogel Culturing. List of all materials used throughout hydrogel culturing, including the vendor, catalog number, lot number, and CAS number, if applicable.

Item Description	Vendor	Catalog Number	Lot Number	CAS#
THP-1	ATCC	TIB-202	70025047	N/A
T-75 Flask	Fisher Scientific	430641U	07120019	N/A
6-well TCP	Fisher Scientific	140675	174211	N/A
Sodium Alginate	Sigma-Aldrich	W201502	MKCC4541	9005-38-3
Calcium Chloride Anhydrous	Thermo Scientific	349615000	A0425202	10043-52-4
Strontium Chloride Anhydrous	Thermo Scientific	012202.36	M17I009	10476-85-4
Magnesium Sulfate	Thermo Scientific	A14491.0I	10246506	10034-99-8
RPMI 1640	ATCC	30-2001		
PMA	Sigma Aldrich	AG-CN2-0010	A00083/B	N/A
LPS	Sigma Aldrich	L3755-100 MG	039M4014V	N/A
PBS 1x	Thermo Scientific	10010-031	2385971	7778-77-0

EDTA Disodium Salt	Thermo Scientific	FL-06-0597	016966	6381-92-6
Sodium Citrate	Thermo Scientific	014K00531	54641	6132-04-3
Sodium Chloride	Fischer Scientific	BP358-1	060877	7647-14-5
PTFE filter details	Thermo Scientific	42225-NN	N/A	N/A

Table A.4 Agarose Plate Preparation. List of all materials used to make agarose plates, including the vendor, catalog number, lot number, and CAS number, if applicable.

Item Description	Vendor	Catalog Number	Lot Number	CAS#
Calcium Chloride Anhydrous	Thermo Scientific	349615000	A0425202	10043-52-4
Strontium Chloride Anhydrous	Thermo Scientific	012202.36	M17I009	10476-85-4
Agarose	Invitrogen	15510-019	073107	9012-36-6
NUNC Petri Dish, 35mm	Fisher Scientific	150255	N/A	N/A
Biopsy 5mm Hole Punch	Fisher Scientific	N/A	P5EXP0218	N/A

Table A.5 SEM Imaging. List of all materials used to prepare hydrogels for SEM imaging, including the vendor, catalog number, lot number, and CAS number, if applicable.

Item Description	Vendor	Catalog Number	Lot Number	CAS#
15 mL conical tube	Thermo Scientific	339650	L3JF3C7116	N/A
50 mL conical tube	Thermo Scientific	430290	18022070	N/A
PBS 1x	Thermo Scientific	10010-031	2385971	7778-77-0
Calcium Chloride Anhydrous	Thermo Scientific	349615000	A0425202	10043-52-4
Strontium Chloride Anhydrous	Thermo Scientific	012202.36	M17I009	10476-85-4
Magnesium Sulfate	Thermo Scientific	A14491.0I	10246506	10034-99-8
Gold/Palladium Coating	Thermo Scientific	089726.03	H17W026	Au: 7440-57-5 Pd: 7440-05-3
Carbon Conductive Tabs	Fisher Scientific	NC9967923	N/A	N/A

Table A.6 Rheometer Measuring. List of all equipment used to measure rheological data of hydrogels, including the vendor, model number, and serial number, if applicable.

Item Description	Vendor	Model Number	Serial #

Haake Mars Modular Advanced Rheometer System	Thermal Fisher	Typ 006-3098	117002127003
Haake Mars Heat Exchanger Z	Thermal Fisher	Typ 003-5375	117001198002
Haake Mars Controller	Thermal Fisher	Typ 006-1385	117002127003
Meβplatte TMP 35 Profiliert	Thermal Fisher	222-1895	1LGA40
Drehkorper/ Rotor P35/Ti/SE	Thermal Fisher	222-2092	02150649

Table A.7 Live/Dead. List of all materials used to perform Live/Dead analysis on hydrogels, including the vendor, catalog number, lot number, and CAS number, if applicable.

Item Description	Vendor	Catalog Number	Lot Number	CAS#
12-well TCP	Fisher Scientific	150628	170907	N/A
6-well TCP	Fisher Scientific	140675	174211	N/A
HBSS	Thermo Scientific	14175-079	2276694	7732-18-5
Calcium Chloride Anhydrous	Thermo Scientific	349615000	A0425202	10043-52-4
Strontium Chloride Anhydrous	Thermo Scientific	012202.36	M17I009	10476-85-4
Magnesium Sulfate	Thermo Scientific	A14491.0I	10246506	10034-99-8
Viability/ Cytotoxicity Kit	Invitrogen	L3224	2506012	N/A

Table A.8 RNA Isolation. List of all materials used to perform RNA isolation of hydrogel encapsulated cells, including the vendor, catalog number, lot number, and CAS number, if applicable.

Item Description	Vendor	Catalog Number	Lot Number	Cas#
TRIzol® Reagent	Thermo Scientific	15596026	424304	N/A
Chloroform	Thermo Scientific	032614.K2	Z17B014	67-66-3
Ethyl Alcohol	Thermo Scientific	111000190	K18A17293	64-17-5
PureLink RNA mini kit	Invitrogen	12183018A	2626710	N/A

Table A.9 RT-PCR. List of all materials used to perform RT-PCR on hydrogel encapsulated cells, including the vendor, catalog number, lot number, and CAS number, if applicable.

Item Description	Vendor	Catalog Number	Lot Number
96-well MicroAmp	Thermo Scientific	4483485	N/A
RNase free water	Thermo Scientific	AM9930	2111165
TaqMan® RT-PCR Mix (2×)	Thermo Scientific	4392587	2709913
Taq Man®RT Enzyme Mix (40×)	Thermo Scientific	4392728	2693481
GAPDH	Thermo Scientific	Hs02786624_g1	1861108
CCR2	Thermo Scientific	Hs00704702_s1	1836679
ITGAM	Thermo Scientific	Hs00167204_m1	1815367
CCR7	Thermo Scientific	Hs01013469_m1	2020942
CD163	Thermo Scientific	Hs00174705_m1	1869600
PCR 8-Tube Strips	Thermo Scientific	P1300	23054

RNAse Away	Thermo Scientific	7002	N/A

Table A.10 ELISA. List of all materials used to perform ELISA on hydrogel encapsulated cell media, including the vendor, catalog number, lot number, and CAS number, if applicable.

Item Description	Vendor	Catalog Number	Lot Number	Cas#
Capture Antibody	R&D	840204	JU1422011	N/A
PBS 1x	Thermo Scientific	10010-031	2385971	7778-77-0
96-well microplate	Falcon	N/A	351172	N/A
Plate Sealers	Flacon	DY992	P305007	N/A
Detection Antibody	Sino Biological Inc.	SEK10139	KW13DE2701	N/A
Conjugated Streptavidin	Ray Biotech Inc.	QA-CY3E	Q0732720	9013-20-1
Streptavidin-HRP	R&D	893975	P335516	9013-20-1
TRIzol Reagent	Life Tech	15596026	424305	N/A
Substrate Reagent Pack	R & D Systems	DY999B	P362226	N/A
Human IL-1beta/IL-1F2	R & D Systems	DY 201-05	P345640	N/A
Human TNF-α	R & D Systems	DY210-05	P302933	N/A
Human CCL2/MCP-1	R & D Systems	DY279	P346423	N/A

Appendix B. Protocols

B.1 Cell Culture

1. Clean the biosafety cabinet and turn on UV light for 30 minutes before the experiment to maintain strict aseptic conditions.
2. Preheat the water bath to 37°C and keep the cryopreserved vial in it for 90 seconds.
3. Quickly remove the vial once thawed and spray it with 70% ethanol for decontamination.
4. Inside the biosafety cabinet transfer the content of the vial to a 15 mL centrifuge tube containing 6 mL of pre-warmed ATCC RPMI cell culture media.
5. Gently pipette mix and then centrifuge at 120 g for 5 minutes at room temperature.
6. Discard the supernatant to get rid of the DMSO.
7. Resuspend the cell pellet in 1 mL of ATCC RPMI cell culture media.
8. Transfer 10 µL of the resuspended cell suspension to a fresh microscope slide and add 10 µL of trypan blue to it.
9. Gently pipette mix the cells with trypan blue and load them on the BioRad^{TM} Cell Counter.
10. Seed all the cells in a single T-75 flask.
11. The total volume of cell culture medium in one T-75 flask will be 15 mL.
12. Allow the cells to grow for two days at 37°C, 95% humidity, and 5% CO2 in the incubator.
13. Replace or add media when necessary:
    i. Add an additional 15 mL of ATCC complete culture media for THP1 cells after 3 days of seeding (these are suspension cells hence, media should be added and not replaced).

14. Once desired cell confluency is attained:
    i. Pellet THP1 cells by centrifuging at 120 g for 5 min and then follow steps 7 to 13 for sub-culturing.

B.2 Preparation of Agarose Plates

1. Prepare 1000 mM $CaCl_2$ and $SrCl_2$ solution in water.
2. Prepare 2.0% Agarose solution in water by heating and mixing the solution until all the agarose has dissolved.
3. Mix equal volumes of $CaCl_2$ or $SrCl_2$ solution with Agarose solution.
    a. The final concentrations should be 500 mM $CaCl_2$ or $SrCl_2$ and 1.0 % Agarose.
4. Autoclave the mixed solution to kill any contamination in the solution.
5. Remove from the autoclave and pour solution into a medium petri dish and allow to gel for 1 hour.
6. After gelling, punch 5mm x 5mm cylinder holes into the gel, about 45 per plate.

B.3 THP1 to Macrophage Differentiation in Hydrogel

1. Prepare 2.0% Alginate in PBS-CM or PBS-SM.
2. Filter 2.0% Alginate through the PTFE filter.
3. Mix THP1 cell solution in 2.0% Alginate so that the final concentration is 1.2% Alginate.
4. Seed 1.2% Alginate solution containing cells in 500 mM $CaCl_2$ or $SrCl_2$ and 1% Agarose plates.
    a. The wells should be 5mm in diameter and 5mm deep.
    b. Volume of cell solution needed per well is 110 µL.
5. Allow hydrogels to form for 30 minutes.
6. Remove hydrogels from 500mM $CaCl_2$ or $SrCl_2$ and 1% Agarose plates and place in 6-well plate containing 4 mL of ATCC RPMI-CM or RPMI-SM cell culture media.
7. Allow the cells to acclimatize for 72 hours and then add 128 ng/mL (100 nM) of PMA working solution to each well of TCP.
8. After 48 hours the expected percentage of cells that got differentiated into M0 macrophages is around 70% to 80%.
9. Aspirate the media from the 6-well plates and wash the wells once with 1x PBS.
10. Now add fresh culture media to the 6-well plate.
11. Allow the cells a resting period of 72 hours at 37°C at 5% CO2 and 95% humidity.
12. After 72 hours, the cells are referred to as M0 rested macrophages.
13. Now add fresh media containing 100 ng/mL of interferon gamma (IFNγ) to the 6-well plates.
14. After 24 hours of incubation, add LPS containing media to the 6-well plates without removing previous media, adjust the

concentration of LPS containing media so that the final concentration for LPS in each well is 100 ng/mL.

15. Allow cells to grow for further 48 hours for their polarization into M1 macrophages.
16. After 48 hours of incubation, aspirate media and add fresh ATCC RPMI-CM or RPMI-SM cell culture media.
17. Repeat step 16 every 72 hours for 12 days.

B.4 SEM Imaging

1. Remove the hydrogel from the media and place it into a 15 mL conical tube.
2. Wash with 1x PBS-CM or PBS-SM.
3. Aspirate PBS out of the conical tube.
4. Place tube containing hydrogels into a -20°C freezer for 3 hours.
5. After 3 hours move the tube to -80°C freezer for 24 hours.
6. Remove conical tube from freezer and lyophilize in -55°C for 24 hours.
7. Remove hydrogels from freeze drier and coat in Au/Pd.
8. Place hydrogel on Scanning Electron Microscope and image at 250x and 2000x at 1kV and 6kV.

B.5 Rheometer Measurements

1. Prepare the HAAKE Mars Modular Advanced Rheometer System by first turning on the air to 1.8 psi.
2. Turn on the Haake Heat Exchanger A water temperature bath.
3. Turn on the Haake Mars Controller unit that powers the rheometer.
4. Turn on the computer and sign in.
5. Insert the Drehkorper/ Rotor P35/Ti/SE into the rheometer.
6. Place the Meβplatte TMP 35 profiliert lower plate onto the rheometer.
7. Select the job 'gelation monitoring.'
8. Adjust parameters to be:
    a. Temperature: 37°C.
    b. Strain: $\gamma = 0.005$
    c. Frequency: 0.1000 Hz
    d. Time: 180 seconds.
    e. Select controlled deformation (CD).
    f. Change gap setting to current gap.
9. Place the hydrogel disc onto the plate and manually lower the probe until it just touches the hydrogel.
10. Start the test and save the results.
11. Repeat steps 9 and 10 for all hydrogels.

B.6 Live Dead Imaging

1. Remove the culture medium covering the hydrogels and replace it with an equal volume of HBSS-CM or HBSS-SM.
2. Prepare a dilute mixture of Component A and Component B dyes by pipetting 1.0 µL of Compound A and 0.5 µL of Compound B into a common 1 mL volume of HBSS-CM or HBSS-SM (1:1000 dilution of Compound A and 1:2000 dilution of Compound B). Mix thoroughly by pipetting up and down several times.
3. Incubate in darkness for 30 minutes at 37℃.
4. Remove the dye solution and wash the cells with fresh HBSS.
5. Incubate at 37℃ for 10 minutes.
6. Replace and incubate 2 more times following steps 4 and 5.
7. Remove hydrogel from media and place on slide.
8. Image hydrogels in GFP and TexasRed.

B.7 RNA Isolation

1. Incubate the lysate with TRIzol® Reagent at room temperature for 5 minutes to allow complete dissociation of nucleoprotein complexes.
2. Add 0.2 mL chloroform per 1 mL TRIzol® Reagent.
3. Shake the tube vigorously by hand for 15 seconds. **Do not Vortex.**
4. Incubate at room temperature for 2 to 3 minutes.
5. Centrifuge the sample at 12,000 × g for 15 minutes at 4°C.
    a. **Note:** After centrifugation, the mixture separates in a lower (red phenol–chloroform phase), an interphase, and an upper (colorless aqueous phase which contains the RNA).
6. Transfer the colorless upper phase containing the RNA to a fresh RNase–free tube.
7. Add an equal volume of 70% ethanol, mix well by vertexing.
8. Invert the tube to disperse any visible precipitate that may form after adding ethanol.
9. Transfer up to 700 µl of sample to a Spin Cartridge (with a Collection Tube).
10. Centrifuge at 12,000 × g for 15 seconds at room temperature.
11. Discard the flow–through and reinsert the Spin Cartridge into the same Collection Tube, repeat steps 9 to 10 until the entire sample has been processed.
12. Add 700 µl Wash Buffer I to the Spin Cartridge.
13. Centrifuge at 12,000 × g for 15 seconds at room temperature.
14. Discard the flow-through and the Collection Tube.
15. Insert the Spin Cartridge into a new Collection Tube.

16. Add 500 µl Wash Buffer II to the Spin Cartridge.
17. Centrifuge at 12,000 × g for 15 seconds at room temperature.
18. Discard the flow–through and reinsert the Spin Cartridge into the same Collection Tube.
19. Repeat steps 16 to 17 once more.
20. Centrifuge the Spin Cartridge and Collection Tube at 12,000 × g for 1 minute at room temperature to dry the membrane with attached RNA.
21. Discard the Collection Tube and insert the Spin Cartridge into a Recovery Tube.
22. Add 30 µl of RNase–Free Water to the center of the Spin Cartridge.
23. Incubate at room temperature for 1 minute.
24. Centrifuge the Spin Cartridge with Recovery Tube for 2 minutes at ≥12,000 × g at room temperature.
25. Repeat steps 22 to 24 two more times (collect all elutes into the same recovery tube).
26. Store your purified RNA on ice for short-term storage hours or at –80°C for long-term storage.
27. Collect data on Quant Studio 3 RNA reading machine.

B.8 RT-PCR

1. Arrange your samples in triplicate for a 96-well format. Results for Real time PCR must be normalized over GAPDH/other (endogenous control).
2. Calculate the number of wells used for each primer including your controls.
3. Using the number above calculate the master mix per primer (GAPDH, CCR2, ITGAM, CCR7, CD163)
4. Set using the table-1 below (Leave out RNA sample this will be added later, so total = 11.5 µL)

Table B.1 Preparation of RT PCR mix for Real time PCR.

Component (Life Technologies Gene Expression Assays)	Volume for one reaction /one well
TaqMan® RT-PCR Mix (2×)	5.0 µL
TaqMan® Gene Expression Assay (20×)	0.5 µL
Taq Man®RT Enzyme Mix (40×)	0.25 µL
RNA sample (50 ng/µL)	x µL
RNase free water	(10 – x) µL
Total volume /well	10 µl

5. Dilute RNA with RNase free water to make the final concentration 10 ng/µL.
6. Aliquot master mix 11.5 µL into the 96-well plate (3 wells per sample).
7. Next add 8.5 µL of 10 ng/µL mRNA to each well of the plate.
8. Cover plate with clear adhesive cover. Be sure that the cover is firmLy attached so that no evaporation occurs during real time process.

9. Spin plate down briefly, so that all reagents are in the well.
10. Set up PCR program as shown in table 2.
11. Set probe #1 to FAM.
12. Set the total volume to 10 µL.
13. Designate each well (primer set and sample type)
14. Mark each set as triplicate wells
15. Set up reaction.
16. Start the PCR program.

Table B.2 Thermal cycling conditions for Real time PCR.

Stage	Step	Temperature (ºC)	Time
Holding	Reverse transcription	48	15min
Holding	Activation of AmpliTaq Gold® DNA Polymerase, Ultra-Pure	95	10min
Cycling (40 cycles)	Denature	95	15 sec
	Anneal/extend	60	1 min

17. Export the data as excel sheet and plot using Graph Pad Prism.

B.9 ELISA

1. Dilute the Capture Antibody to the working concentration in PBS without carrier protein.
2. Immediately coat a 96-well microplate with 100 µl per well of the diluted Capture Antibody.
3. Seal the plate and incubate overnight at room temperature.
4. Aspirate each well and wash with Wash Buffer, repeating the process two times for a total of three washes. Wash by filling each well with Wash Buffer (400 µL) using a squirt bottle.
5. Complete removal of liquid at each step is essential for good performance. After the last wash, remove any remaining Wash Buffer by aspirating.
6. Block plates by adding 300 µL Reagent Diluent to each well. Incubate at room temperature for a minimum of 1 hour.
7. Repeat the aspiration/wash steps (step 4 to 5).
8. Add 100 µL of sample or standards in Reagent Diluent, or an appropriate diluent, per well.
9. Cover with an adhesive strip and incubate for 2 hours at room temperature.
10. Repeat the aspiration/wash steps (step 4 to 5).
11. Add 100 µL of the Detection Antibody, diluted in Reagent Diluent, to each well.
12. Cover with a new adhesive strip and incubate for 2 hours at room temperature.
13. Repeat the aspiration/wash steps (step 4 to 5).
14. Add 100 µL of the working dilution of Streptavidin-HRP to each well.
15. Cover the plate and incubate for 20 minutes at room temperature. Avoid placing the plate in direct light.
16. Repeat the aspiration/wash steps (step 4 to 5).

17. Add 100 µL of Substrate Solution to each well. Incubate for 20 minutes at room temperature. Avoid placing the plate in direct light.
18. Add 50 µL of Stop Solution to each well. Gently tap the plate to ensure thorough mixing.
19. Determine the optical density of each well immediately, using a microplate reader set to 450 nm.
20. Export the file on computer as excel sheet.
21. Visit https://www.arigobio.com/elisa-analysis.
22. Upload the OD raw data and define the wells and standards.
23. Analyze the data to get the concentrations of your unknown samples.
24. Plot the data in Mean ± Standard Deviation plot using Graph Pad Prism.